LAPPEENRANTA
UNIVERSITY OF TECHNOLOGY

Kimmo Järvinen

DEVELOPMENT OF FILTER MEDIA TREATMENTS FOR LIQUID FILTRATION

Thesis for the degree of Doctor of Science (Technology) to be presented with the due permission for public examintion and criticism in the Auditorium 1382 at Lappeenranta University of Technology, Finland, on the 9th of December, 2005, at noon.

Acta Universitatis
Lappeenrantaensis
227

Supervisor	Professor Lars Nyström Department of Chemical Technology Lappeenranta University of Technology Finland
Reviewers	Dr. Steve Tarleton Department of Chemical Engineering Loughburouhg University UK
	Professor Wilhelm Höflinger Vienna University of Technology Austria
Opponent	Professor Wilhelm Höflinger Vienna University of Technology Austria
Custos	Professor Lars Nyström Department of Chemical Technology Lappeenranta University of Technology Finland

ISBN 952-214-137-2
ISBN 952-214-160-7 (PDF)
ISSN 1456-4491

Lappeenrannan teknillinen yliopisto
Digipaino 2005

ABSTRACT

Kimmo Järvinen
Development of filter media treatments for liquid filtration
Lappeenranta 2005
75 pages, 22 figures, 10 tables, 7 appendices
Acta Universitatis Lappeenrantaensis 227
Diss. Lappeenranta University of Technology
ISBN 952-214-137-2, ISBN 952-214-160-7 (PDF)
ISSN 1456-4491

Woven monofilament, multifilament, and spun yarn filter media have long been the standard media in liquid filtration equipment. While the energy for a solid-liquid separation process is determined by the engineering work, it is the interface between the slurry and the equipment - the filter media - that greatly affects the performance characteristics of the unit operation. Those skilled in the art are well aware that a poorly designed filter medium may endanger the whole operation, whereas well-performing filter media can make the operation smooth and economical.

As the mineral and pulp producers seek to produce ever finer and more refined fractions of their products, it is becoming increasingly important to be able to dewater slurries with average particle sizes around 1 µm using conventional, high-capacity filtration equipment. Furthermore, the surface properties of the media must not allow sticky and adhesive particles to adhere to the media.

The aim of this thesis was to test how the dirt-repellency, electrical resistance and high-pressure filtration performance of selected woven filter media can be improved by modifying the fabric or yarn with coating, chemical treatment and calendering.

The results achieved by chemical surface treatments clearly show that the woven media surface properties can be modified to achieve lower electrical resistance and improved dirt-repellency. The main challenge with the chemical treatments is the abrasion resistance and, while the experimental results indicate that the treatment is sufficiently permanent to resist standard weathering conditions, they may still prove to be inadequately strong in terms of actual use.

From the pressure filtration studies in this work, it seems obvious that the conventional woven multifilament fabrics still perform surprisingly well against the coated media in terms of filtrate clarity and cake build-up. Especially in cases where the feed slurry concentration was low and the pressures moderate, the conventional media seemed to outperform the coated media. In the cases where the feed slurry concentration was high, the tightly woven media performed well against the monofilament reference fabrics, but seemed to do worse than some of the coated media. This result is somewhat surprising in that the high initial specific resistance of the coated media would suggest that the media will blind more easily than the plain woven media. The results indicate, however, that it is actually the woven media that gradually clogs during the coarse of filtration. In conclusion, it seems obvious that there is a pressure limit above which the woven media looses its capacity to keep the solid particles from penetrating the structure.

This finding suggests that for extreme pressures the only foreseeable solution is the coated fabrics supported by a strong enough woven fabric to hold the structure together. Having said that, the high pressure filtration process seems to follow somewhat different laws than the more conventional processes. Based on the results, it may well be that the role of the cloth is most of all to support the cake, and the main performance-determining factor is a long life time.

Measuring the pore size distribution with a commercially available porometer gives a fairly accurate picture of the pore size distribution of a fabric, but fails to give insight into which of the pore sizes is the most important in determining the flow through the fabric. Historically air, and sometimes water, permeability measures have been the standard in evaluating media filtration performance including particle retention. Permeability, however, is a function of a multitude of variables and does not directly allow the estimation of the effective pore size.

In this study a new method for estimating the effective pore size and open pore area in a densely woven multifilament fabric was developed. The method combines a simplified equation of the electrical resistance of fabric with the Hagen-Poiseuille flow equation to estimate the effective pore size of a fabric and the total open area of pores. The results are validated by comparison to the measured values of the largest pore size (Bubble point) and the average pore size. The results show good correlation with measured values. However, the measured and estimated values tend to diverge in high weft density fabrics. This phenomenon is thought to be a result of a more tortuous flow path of denser fabrics, and could most probably be cured by using another value for the tortuosity factor.

Keywords: Coated filtration fabrics, Liquid filtration, Fabric open area, effective pore size

UDC 66.067.12

PREFACE

The work for this dissertation was carried out in the Department of Chemical Technology at Lappeenranta University of Technology and Tamfelt Corp. Filter Fabric Division's R&D department between 1999 to 2005.

I wish to express my gratitude to Professor Lars Nyström for his invaluable advice and fatherly patience during the years we have worked together on research. I also wish to thank professors Marja Oja and Matti Lindström for their assistance and encouragement in the experimental and modelling work for the study. The other members for my study, Mr. Jani Hämäläinen, Ms. Arja Puolakka, Mr. Aarne-Matti Heikkilä, Mr. Pertti Rantala, and Ms. Kati Toitturi, I would like to thank for their collaboration. I am grateful to the members of Filter fabric Division and especially to its former and present leaders, Msrs. Esko Pessi and Heikki Rehakka, for providing me with the resources which enabled me to carry out the experimental part of the study.

I wish to thank Dr. Steve Tarleton and Dr. Wilhelm Höflinger for their constructive comments and guidance. Throughout the years, I have been privileged to be able to rely on Mr. Esko Lahdenperä's friendly advice and guidance on process simulation and numerical analysis methods.

Special thanks go to The National Technology Agency of Finland (FIN) and The Federation of Finnish Textile and Clothing Industries (FIN) for supplying project funding and support.

Most of all, I am grateful to my wife Teija and my sons Sampo and Antti for their constant patience and support, and I would like to dedicate this thesis to them. I would also like to give special thanks to my parents, Leila and Pentti, for their encouragement throughout the work.

Tampere, October 2005
Kimmo Järvinen

LIST OF PUBLICATIONS

The experimental part of this thesis is based on the papers I-VII. Throughout this text these publications will be referred to by their Roman numerals.

Appendix I
Järvinen K., A novel technique for estimating the effective pore size and open area for densely woven filter fabrics, Filtration, 5(2), 2005, pp.126-133.

Appendix II
Järvinen K, Toitturi K., Oja M., Development of Microfiltration Medium: Testing of Filter Cloths for Dead-end Submicron Filtration, Proceedings of the International Technical Conference on Filtration and Separation, March 14-17, 2000 Myrtle Beach, South Carolina.

Appendix III
Järvinen K, Oja M., Rantala P., Development of high pressure filtration cloths, Filtration 5(4), 2005, pp 295-304.

Appendix IV
Järvinen K., Hämäläinen J., Dirt-Repellant Fabrics for Deinked Pulp Dewatering Processes, Filtration 3(3), 2003, pp 139-142.

Appendix V
Järvinen K., Heikkilä A-M., Filtration cloth for solid liquid systems, WO Patent 02/074416 A1.

Appendix VI
Järvinen K., Puolakka A., Weathering of Polyaniline-Treated Polyester Filter Fabrics, Textile Research Journal, Vol. 7, July 2003, pp. 593-596.

Appendix VII
Järvinen K., New Diaphragm Media for Nickel Electrowinning Processes, Technical Proceedings of the ALTA 2003 Nickel/Cobalt Conference, Published by ALTA Metallurgical Services, Melbourne, Australia.

Own contribution in publications

Appendix I: A novel technique for estimating the effective pore size and open area for densely woven filter fabrics. Designing, planning and supervising the media manufacturing and analytical work, joint theoretical development work with professor Matti Lindström, pore size distribution analysis, conclusions and paper preparation.

Appendix II: Development of Microfiltration Medium: Testing of Filter Cloths for Dead-end Submicron Filtration. Designing, planning and supervising the experimental work and related masters thesis work, preparation of the paper and drawing the final conclusions, presenting the paper in Myrtle Beach.

Appendix III: Development of high pressure filtration cloths. Designing, planning and supervising the experimental work, drawing the final conclusions and preparation of the paper published in Filtration.

Appendix IV: Fabrics for De-inked Pulp Dewatering Processes. Planning and supervision of the experimental work, filter cloth design, drawing the final conclusions and preparation of the paper published in Filtration.

Appendix V: Filtration cloth for solid liquid systems. Combining the known technology of manufacturing conductive fabrics with the knowledge about filtration fabrics. Conductive filter cloth design and related development of manufacturing process, designing and operating the pilot-scale experimental apparatus, preparing the patent text.

Appendix VI: Weathering of Polyaniline-Treated Polyester Filter Fabrics. Filter cloth design, manufacturing supervision, planning and supervising the experimental work, preparation of the paper and drawing the final conclusions

Appendix VII: New Diaphragm Media for Nickel Electrowinning Processes. Planning and supervising the media manufacturing and test run analytical work, design of test fabrics, paper preparation and conclusions, presenting the paper in Perth, Australia.

CONTENTS

Nomenclature

Alphabets (capital)

A	cross sectional area of the medium, m^2
A_e	effective open area of the medium, m^2
A_0	Cross sectional open area of the medium, m^2
AP	measured air permeability, m^3m^{-2} s^{-1}
C	numerical parameters for pore shape, dimensionless
C_D	orifice discharge coefficient for wire media, dimensionless
CF	cover factor by Peirce, surface area coverned by yarns, dimensionless
D_i	diffusivity of ionic species i, m^2s^{-1}
E^0	standard electrode potential, V
F	Faraday's constant (96487 C/eq)
H	temperature, K
I	current, A
I_A	current density, Am^{-2}
I_c	measured cell current with cloth, A
I_0	measured cell current without cloth, A
K	Kozeny constant, dimensionless
K_0	pressure drop coefficient, dimensionless
K_1	pressure drop coefficient, dimensionless
K_2	pressure drop coefficient, dimensionless
L	thickness of media, m
L_c	thickness of cake, m
M	kinetic energy loss coefficient, dimensionless
N	viscous energy loss coefficient, dimensionless
N_0	number of openings per unit area, number m^{-2}
Q	velocity of fluid, m s^{-1}
R	universal gas constant (8.3145 J K^{-1} mol^{-1})
R_H	hydraulic radius of a pore of a medium, m
R_m	resistance of the medium, m^{-1}
R_{mf}	apparent medium resistance, m^{-1}
R_p	resistance of the pores, m^{-1}
R_y	resistance of the yarns, m^{-1}
Re	Reynolds number, dimensionless
S	specific surface, m^2m^{-3}
S_0	open pore specific surface, m^2m^{-3}
S_f	external surface area, m^{-1}
S_{perc}	percentage of mercury saturation in a media, %
S_1	weft yarn shortening percentage, %
S_2	warp yarn shortening percentage, %
T	yarn linear density (fineness), tex
T_1	weft yarn linear density, tex
T_2	warp yarn linear density, tex
U	cell voltage, V
U_c	test cell voltage with fabric, V
U_o	test fluid voltage without fabric, V
V	filtrate volume, m^{-3}
V_s	volume of filtrate collected before constant filtration pressure, m^3
W	wetted orifice perimeter for wire media, m

Alphabets (lower case)

a	empirical constant, dimensionless
b	empirical constant, dimensionless
c	effective concentration of solids in the feed, % w/w or kg m^{-3}
c_i	concentration of ionic species or component, mol/l
d	media pore diameter, m
d_f	diameter of particulate bed single particle, m
d_p	mean particle size, m
d_y	yarn diameter, m
$d_{p,\ eff}$	effective media pore diameter, m
d_1	diameter of weft yarn, m
d_2	diameter of warp yarn, m
j	flux of species *i* through the diaphragm cloth, mol s^{-1}
k	permeability, m^2
k_m	permeability of a cloth if made of monofilaments, cm^2
k_y	permeability of the yarns in a cloth, cm^2
k_0	permeability factor, m^2
l	length of capillary, m
l_0	fibre length, m
m	exponent, dimensionless
m_{dc}	mass of dry cake, kg
m_{wc}	mass of wet cake, kg
n	compressibility coefficient, dimensionless
n_p	number of pores in media, count number
Δp	pressure difference, Pa
Δp_c	pressure difference over a filter cake, Pa
p	pressure, Pa
p_d	extrapolated pressure, Pa
p_L	liquid pressure, Pa
p_s	compressive drag pressure acting on a solids in a filter cake, Pa
p_1	pressure difference over the medium, Pa
q	superficial flow rate of fluid, $m^3m^{-2}s^{-1}$
s_1	sett of weft yarns, number of weft yarns per centimeter
s_2	sett of warp yarns, number of warp yarns per centimeter
r	capillary radii, m
t	time, s
t_s	time before constant filtration pressure, s
v	bulk flow in the voids of the medium, $m^3m^{-2}s^{-1}$
x	distance coordinate into a medium or diaphragm, m
w	specific planar weight of a media, gm^{-2}
w_m	mass of dry solids deposited per unit area, kgm^{-2}
z	charge of species i, dimensionless

Greek Symbols

α	specific resistance of a filter cake, m kg^{-1}
α_{av}	specific resistance of a filter cake averaged over the compressive drag stress, m kg^{-1}
β	ratio of multifilament yarn media permeability to monofilament yarn media permeability, dimensionless
Ω	ratio of the electrical resistivity of the saturated porous medium to that of the fluid, dimensionless
Ω_m	media electrical resistance, Ohms
Ω_y	yarn material electrical resistance, Ohms
Ω_p	liquid filled pores electrical resistance, Ohms
κ	conductivity of the fluid, S m^{-1}
κ_p	conductivity of the medium, S m^{-1}
μ	fluid viscosity, Pa s
θ	contact angle between pore wall and fluid, degree
ρ	fluid density, kg/m^3
ρ_s	solids density, kg/m^3
ρ_f	fiber (polymer) density, g cm^{-3}
ρ_p	bulk density of a cloth, g cm^{-3}
ρ_y	yarn true density, g cm^{-3}
ρ_{1f}	weft yarn true density, g cm^{-3}
ρ_{2f}	warp yarn true density, g cm^{-3}
σ	surface tension of fluid,
τ	tortuosity factor, dimensionless
φ	porosity, dimensionless
φ_c	cake porosity, dimensionless
φ_d	density porosity, dimensionless
φ_y	yarn porosity (intrayarn porosity), dimensionless
φ_p	interyarn porosity, dimensionless
φ_{Hw}	media porosity based on hydraulic pore model, dimensionless
ξ	parameter defined by eq. 4.4.2.

Abbreviations

AP	Measured air permability, $m^3m^{-2}s^{-1}$
C-P cell	Compressibility-Permeability test Cell
ePTFE	Expanded Polytetrafluoroethylene
GCC	Ground Calcium Carbonate
PBT	Polybutylene Terephtalate
PCC	Precipitated Calcium Carbonate
PET	Polyethylene Terepthalate (polyester)
PMI	Porous Materials Inc.
PP	Polypropylene
PA	Polyamide
PTFE	Polytetrafluoroethylene
PU	Polyurethane
PVDF	Polyvinylidene Fluoride
Nylon 6.6	Polyhexamethylene-adipamide
SiC	Silicone carbide

1 Introduction

Filter cloth is often thought to be the heart and soul of filtration equipment. Although, as stated by Mayer [1] and Tiller [2], cake filtration is just one part of solid-liquid-separation (SLS) technology, and the role of filter media is most important in the early stages of filtration when the cake is formed, being able to design a filtration fabric with good resistance to blinding (prerequisite for long medium life), desired permeability and pore size distribution is one of the main challenges for a filter media designer.

For heavy duty solid-liquid separation equipment, most of the filtration media utilised today are manufactured with conventional weaving technology, using reinforced weaving looms and, in some cases, heat-setting and calendering equipment. Even the most state-of-the-art heavy duty tower presses, high-pressure tube presses and twin wire presses use woven fabrics made out of mono- or multifilaments. [3]

The most important design variables for a woven fabric are yarn type (polymeric material, filament or staple, diameter, construction, twist type) in the warp and weft directions, weave structure, yarn sett and finishing. From these parameters, if the weaving machine particulars and finishing instructions are known, the main characteristics of the performance of filtration fabric, that is to say, mechanical strength, thickness, durability (life), particle capture, permeability and porosity could be estimated.

Assuming that the weaving and finishing processes do not damage the yarns, the mechanical strength of a fabric can be estimated simply by summing up the individual yarn strengths in warp and weft directions. The thickness of a fabric depends mainly on the weave type used, single layer fabrics having a thickness roughly equal to the diameter of a single yarn, double layer fabrics having a thickness equal to double the single yarn diameter, and so on.

In cake filtration, particle capture and cake build-up capacity are mainly determined by the number, size and shape of the pores of the media. Although the pores can sometimes be more than ten times wider than the particle size to be captured due to bridging effect, the

size and shape of pores is nevertheless the main determining factor, together with the overall permeability, in desired particle capture and cake build-up performance. [7]

Originally the cover factor calculations were developed to help the apparel fabric designers to compare such things as different designs in terms of fabric weight, dyeability, cost and feel, but they also made it possible to predict the porosity and water and air permeability of different designs. Many of the basic assumptions, however, that have to be made in making the cover factor calculations (for example, round yarn diameter, incompressible yarns and 100 % solid yarns) systematically result in higher cover factors (that is to say, lower porosity) than the actual fabrics have. Yet another, maybe much more significant limitation, is the absence of the surface properties of yarn which affect the filtration performance of any fabric and design. [10], [11]

The advantages of the conventional woven fabrics over non-woven or other more modern structures are mostly related to the mechanical strength, abrasion resistance and durability, not necessarily to the actual fluid dynamical performance. It can be foreseen that, for many applications, it would be beneficial to take advantage of modern inventions in polymer science in order to improve the medium performance, if mechanical durability permitted this. With existing technology having been explored and optimised for years, however, it is very difficult to find new, high-performance technologies at competitive manufacturing costs.

Interestingly enough, the theory behind the design and optimisation of a particular medium design is still partly lacking when it comes to the designer's ability to predict the effective pore size of a particular yarn and weave pattern. While there exist many theories and empirical formulae to calculate the open pore size and shape of monofilament yarn-based woven fabrics, the practical value of most theories is low when it comes to the design of tightly woven fabrics using multifilament or spun yarns.

Very few mathematical tools are presented in literature when it comes to predicting the permeability and pore size distribution of a woven fabric based on the actual design parameters, such as yarn count, weave and fabric finish. Many of the existing models are based on fluid flow through glass spheres of porous media or sand. These models, while valid and useful for deep-bed filtration applications, do not adequately apply to thin, tightly

woven multifilament and/or spun yarn fabric structures. Even the best of the models developed for woven monofilament fabrics or non-wovens do not allow sufficiently good prediction of the characteristics of tightly woven multifilament fabrics. Moreover, some of the models are simply too complicated to be used in industrial manufacturing. [42]

2 Filter media design and manufacturing

This literature review is a summary of the basic principles of manufacturing a woven solid-liquid filtration medium, coated and non-coated, used in the experimental part of the thesis.

In the past few centuries, many handbook-type textbooks on technical textiles manufacturing have been published, such as Horrocks and Anand's Handbook of Technical Textiles [4] and Adanur's Wellington Sears Handbook of Industrial Textiles [5]. A much more focused view of technical textiles as filter media, a view maybe sometimes too restricted for R&D use, but nonetheless a view of the technical textiles as filter media, is given in Purchas's Handbook of Filter Media [6] and Rushton, Ward, and Holdich's Solid-Liquid Filtration and Separation Technology [7].

2.1 Design fundamentals of woven filter media

The conventional definition of a textile is a woven fabric, or a cloth, which has been made by the process of weaving on a loom. Cloths of different patterns are produced on the loom by varying the manner in which the warp and weft yarns are woven together. The warp yarn is stretched in the machine in a longitudinal direction and the weft yarn lies at right angles to the warp. The most typical weave patterns and the ones used in the present work, namely plain, twill and satin, are illustrated in figure 2.1.1.

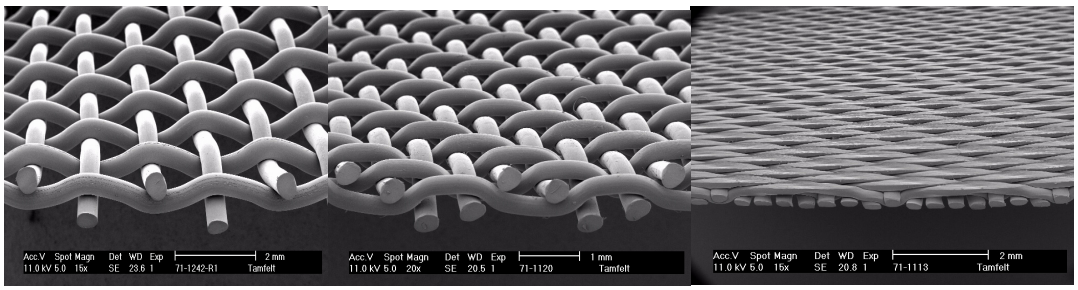

plain weave 2/2 twill weave 7/1 satin weave

FIG 2.1.1. Most typical weave patterns in woven mono- and multifilament cloths.

As shown for example by the studies of Lu *et al.* [8] and Rushton and Rushton [9], the weave pattern has a significant effect on cake formation and consequently on filtration performance in solid-liquid filtration.

The optimal structure of a particular woven filter cloth depends on the application of the fabric and the type of yarn used in weaving. Until the advent of synthetic fibres, the only fibres available to the filter fabric manufacturer were those of natural origin, principally cotton. The ability of cotton to swell when wet makes for a highly retentive filter fabric and, for this reason, cotton is used in some specific applications even today.

Due to its generally poor chemical resistance, however, cotton was firstly replaced by polyamide 6.6 (nylon), a polymer with superior resistance to chemical conditions and mechanical stress. Nylon was followed by polyethylene terephthalate (PET) that offered considerably better resistance to acidic environments, although it offered relatively poor resistance to alkalis and hydrolytic conditions. Even tougher, smoother polymers such as nylon 11 and 12 and similarly polybutylene terephthalate (PBT) were developed to provide superior toughness and resistance to alkalis. Today, by far the most widely used polymer in liquid filtration is polypropylene (PP). The reasons for this are simple; it offers much greater resistance to a wider range of chemical conditions, it can be converted into a variety of thread styles and it is relatively inexpensive due to its large production volume.

All of the above synthetic polymers are available in a multitude of yarn forms: monofilament, multifilament, staple fibre and numerous mixtures of the same and several different kinds of polymeric materials.

Monofilament yarns are produced by extruding molten polymer through a specially engineered die or spinneret. The filaments are then drawn through a series of rollers so as to orientate the molecules and thereby develop the desired stress/strain characteristics. Monofilament yarns used in solid-liquid filtration fabrics typically vary from 0.1 up to 1.2 mm in diameter. The shape of the yarn is not necessarily round; rectangular (or flat) yarns have also been successfully used in liquid filtration fabrics. Chemical and surface properties (hydrophilicity/hydrophobicity) are the main factors determining the choice of yarn raw material for a specific application, whereas the mechanical forces extended by

the filtration equipment to the fabric (tension, compression) and the rheology of the slurry to be filtered determine the size of yarn and the fabric structure.

For monofilament cloths, the range of pore size is from 5,000 to about 30 μm, the lower limit being determined by the size of fibre available for the weaving process. These cloths (sometimes called wire in the pulp and paper industry) are characterised by visually detectable open pores, which create little flow resistance. For monofilament fabrics many applications are found in areas where high throughput is required, such as in the oil, paint, pulp & paper and water purification industries. These cloths are usually easily cleaned by back-flushing.

In the pulp and paper machine industry, the modern trend is to produce composite weaves from fine and coarse monofilaments, in order to have good cake release properties and non-blinding characteristics on the surface layer, and mechanically strong support and a drainage layer on the backside of the cloth. In effect these cloths are designed to simulate the combination of a top-filtering cloth supported by a backing cloth. To combine good cake release with high dewatering capacity, it is advantageous to combine yarns of different diameters for the production of multilayered fabrics as presented in Figure. 2.1.2.

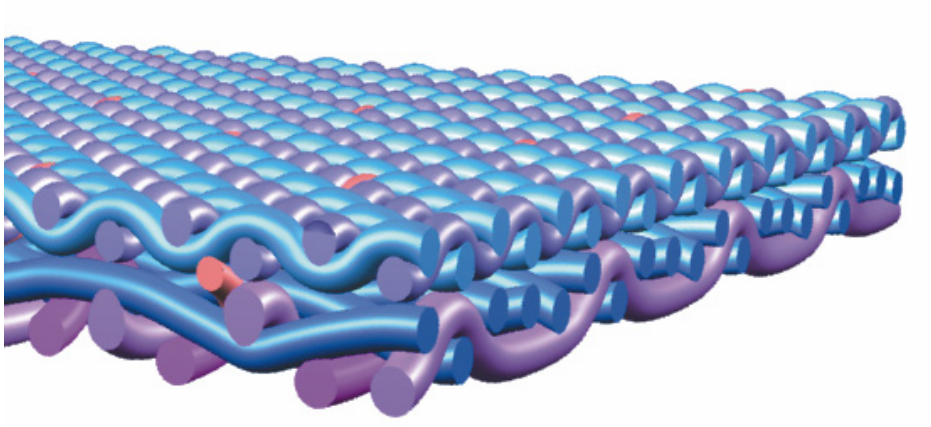

FIG 2.1.2. Typical multilayer paper machine formation fabric by Tamfelt Corp..

Multifilaments are produced in much the same way as monofilaments, except that the spinneret has a multiplicity of much finer holes so as to produce simultaneously a corresponding number of filaments of about 6 μm in diameter. For polymeric staple fibre yarn production, the extruded long fibres have to be first chopped into short pieces of some 40 to 100 mm in length and then spun into yarns using the spinning techniques originally developed for the processing of natural fibres such as 40-50 mm cotton fibres. Multifilament yarns usually have to be intermingled or twisted together in order to facilitate weaving, as shown in Figure. 2.1.3. [5]

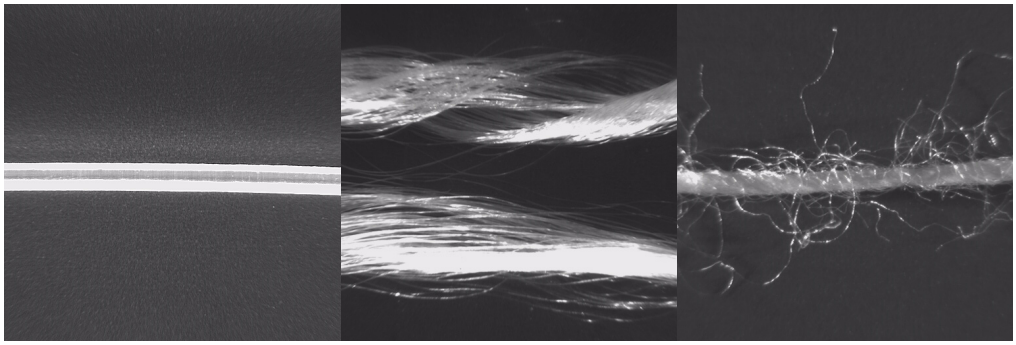

Monofilament yarn Multifilament yarn Spun yarn

FIG 2.1.3. The three standard types of yarn; monofilament, multifilament and spun yarn.

In practice, it is usual to identify the size of fine filaments in terms of denier, tex or decitex, which define the weight of a standard length of filament (also referred to as yarn linear density), and so depend on the density of yarn polymer. Definitions of yarn linear density are:

denier = the weight in grammes of 9,000 metres of filament
decitex(detx) = the weight in grammes of 10,000 metres of filament
tex = the weight in grammes of 1,000 metres of filament

Kienbaum [12], among others, uses the following generalised equation for calculating the diameter of a yarn based on the known yarn linear density T and fibre density ρ_f.

$$d_y = \sqrt{\frac{4\,T}{1000\pi\rho_f\varphi_y}} \qquad (2.1.1)$$

For solid monofilament yarns, the yarn packing (equivalent to porosity) φ_y equals one. For multifilament yarns, the packing depends on such things as the number of filaments, level of twist, fibre length, fibre diameter and compression. For a moderate level of twist, it has been empirically found [13] that

$$\varphi_y = \frac{\rho_y}{\rho_f} \approx 0.525 \qquad (2.1.2)$$

Filtration fabrics produced from continuous multifilament yarns are generally more flexible and stronger and consequently more suitable for use in high-pressure filtration equipment. Having one hundred or more thin filament yarns twisted together strengthens the yarn and makes it more rigid, whilst also helping to protect it from abrasion both during weaving and filtration. Although staple fibre yarns are clearly inferior in terms of mechanical strength, it has been claimed that they are better for certain filtration applications than multifilament yarns, at least in two respects: in providing a higher throughput and in being less prone to blinding due to the higher porosity of the yarns.

The weight of multifilament cloths for solid-liquid filtration can vary considerably, from 2,000 g m^{-2} or more, down to about 300 g m^{-2}. Thanks to their flexibility and mechanical strength, it is possible to weave multifilament yarns tightly enough to enable medium-pore openings of less than 10 µm as shown by Järvinen [15].

In the textile industry, the cover factor calculation by Pierce [14] is commonly used to estimate the area covered by the projection of yarns

$$CF = \frac{d_1}{s_1} + \frac{d_2}{s_2} - \frac{d_1 d_2}{s_1 s_2} \qquad (2.1.3)$$

Where d_1 and d_2 are weft and warp yarn diameters respectively, s_1 and s_2 are the respective setts (a term used to indicate the spacings of ends or picks or both in a woven cloth expressed as threads per centimetre). The cover factor is basically the reverse of

the total open area used in the filtration industry. The fact that the yarns bend significantly, however, and may also compress during the weaving operation, limits the use of the cover factor calculation as an estimate of the total open area.

If the fabric thickness *L* and planar weight *w* could be measured accurately, the density porosity could be evaluated simply as:

$$\varphi_d = \frac{w}{\rho_f L} \tag{2.1.4}$$

Density porosity is equivalent to the total porosity of the fabric including the yarn surface valleys and dead-end pores. Consequently, the porosity available for fluid flow is less than the density porosity.

A well-proven technique for the manufacturing of solid-liquid separation media for certain specific applications is the combination of woven fabric with the well-established technique of needle-punching. Before needling, the web of loose fibres is prepared with great care, using the traditional carding methods of the textile industry; several layers of carded fibre are stacked on top of each other, according to the desired thickness and density of the final needle felt. Carding aligns the fibres along the length of the machine, so that a stack of layers in parallel produces a felt, which is far stronger in the machine direction than transversely. Cross-laying of alternative layers can eliminate this directional difference, or even reverse it, depending on the angle between consecutive layers. For most solid-liquid filtration equipment, it is necessary to strengthen the felt by needling it around an inner monofilament woven fabric or extruded scrim, which is basically a single-layer open mesh. [17], [19]

The competing technology of producing fabrics is broadly named as “non-woven” referring to various adhesive techniques such as adhesive dispersion, wet- and dry-laying of fibrous webs, and bonding with thermoplastic fibres. Alternatives also involve mechanical bonding, based on needling, or stitch-knitting with or without the use of binding threads.

The most recent, and maybe the most interesting techniques from the filtration media development point-of-view, are the steadily increasing possibility to laminate two or more

different fabrics to each other, or to apply a coating to a woven or non-woven fabric, so as to form a composite product.

To aid in the selection of filter cloth, plenty of tabulated and fuzzy information has been presented, usually by the media manufacturers for commercial purposes [3], [16]. As very correctly pointed out by Rushton *et al.* [7], however, it is practically impossible to select a good cloth without reference to the slurry being processed. In the end of course, the best test method is the installation of potential media in an operation unit. This type of study will produce relevant information on wear resistance, cloth life expectancy, cake release and other factors, which are difficult to predict with certainty from other test methods.

2.2 Modifying yarn and fabric chemistry for anti-contaminant properties

Interest in the surface finishing and modification processes for fabric filter began in the late 1960s and early 1970s. It coincided with the introduction of synthetic media for use in industrial filters because such media were easier to modify, and lent themselves to finishing technologies. [21]

As mentioned earlier, most synthetic polymers have limitations in terms of chemical and/or mechanical resistance. Consequently, new yarns, fabrics and surface treatments are continuously being developed by manufacturers aiming to extend media life and improve particle retention, cake release and filtrate drainage.

The strength of adhesion, better known as soiling in the pulp and paper industry, of contaminants present in the filtration process, depends on the interactive forces between the yarn surface and the contaminants. They can be either pure mechanical adhesion or adsorption processes. In the latter case, the hydrophobic and/or hydrophilic interactions are responsible for the adhesion. Stickies in the de-inking processes most often attach to the fabric surface through relatively weak van der Waals forces, which means that the contaminants have to be able to come very close to the fabric surface. The soiling weakens dewatering and causes local differences in porosity, as well as shortening fabric life. All these result in problems in paper quality and machine runnability. [27]

Chemical treatments have been successfully used to modify both the electrochemical and physical nature of the surface of the forming fabrics and, as a result, they have been effective in reducing fabric contamination. If the fabric is finished with, say, silicone or fluorochemical treatment, water diffusion at the boundary surface is possible, and the degree of electrochemical bonding between contaminant and yarns is reduced. Practical experiences confirm that the main problem with dirt repellent treatments is that the high-pressure showers and/or slurry acidic/alkalic chemicals usually wash the treatment away in a relatively short time. [30]

Another approach is to blend surface energy-lowering polymers to the master batch in yarn extrusion process. If abrasion occurs during the running life of the fabric, the fabric continues to retain its anti-contaminant behaviour. Yarn manufacturers have tested various polymer mixtures, such as silicone and polyolefins, but the best results have been achieved with fluoropolymers. By adding high percentages of fluoropolymers or poly-ethylene to pure polyester, however, the strength decreases slightly, elongation increases somewhat and thermal shrinkage varies minimally. Hydrolysis and dry-heat resistance are somewhat higher. [28], [29], [30], [31]

Traditionally, electrochemical modification of yarn properties has been achieved by doping the polymer with metal salts or carbon material during yarn production, or as a separate fibre/filament in the yarn preparation stage. Alloying polyester and other synthetic yarns, however, have the tendency to deteriorate the mechanical properties of the yarn [32].

Giving a ready-made fabric a conductive finish has been studied by several authors [33], [36]. Polyaniline in its doped form is electrically conductive. This type of polyaniline is soluble in organic solvents, for example toluene and xylene. Polyaniline solutions can be used, for example, to treat a filtration fabric to improve its performance in various filtration applications [34]. Compared to traditional antistatic filtration fabrics, the polyester fabrics treated with polyaniline can be more easily used in the sewing of various types of filtration cloths and bags. Typically the conductivity of the treated fabrics varies in the range of 10^4 $–10^9$ S cm^{-1}. [35], [37]

2.3 Calendering and coating woven solid-liquid filtration media

The calendering process improves the surface smoothness of the fabric, and therefore its cake release capability, but also regulates the fabric's permeability and open pore size, and therefore its filtration efficiency. Calendering is achieved by passing the fabric between heated, pressurised rollers, using temperature, pressure and speed as control parameters. A well-known disadvantage of calendaring, however, is that it may result in a reduced surface area of open pores and consequently reduced throughput. [18], [21]

Air filtration and membrane technologies are probably the closest sources of technological innovations in searching for suitable chemical treatment and coating technologies for liquid filtration applications.

For air filtration applications, it is customary to improve the surface smoothness and particle capture of woven/non-woven media by bonding, laminating, coating or impregnating an additional layer on top of the substrate [20]. As early as 1973, W.L. Gore *et al.* and associates started to produce expanded polytetrafluoroethylene (ePTFE) membranes that were applied to a needlefelt support for dust filtration applications. With the expiry of some intellectual property of Gore, several new producers have entered the market and developed the technology further for air filtration applications. [6]

Although membrane technology has made great progress in cross-flow microporous media manufacturing in the past few decades, and although synthetic polymers like polyvinylidene difluoride (PVDF) and polytetrafluoroethylene (PTFE) are commonly used to produce submicron-rated media for the purification of colloidal particles, such as bacteria, fibres, semiconductors and other low-concentration material purification, most of the bonding, laminating, coating and impregnating techniques used today by the filtration media manufacturers are still for the purposes of air and dust filtration. [22], [23]

For conventional heavy-duty solid-liquid separation processes, the tensile strength requirement of media is typically higher than 55 N m^{-1}, combined with low longitudinal

expansion. For submicron particle capture, however, the traditional monofilament woven fabrics are limited to an open pore diameter of approx. 24 µm. Multifilament fabrics or fabric-reinforced felts could potentially be used in fine particle capture because it is possible to weave a fabric down to a 10 µm rating, but their limitation in the form of irreversible clogging may sometimes impair the filter function after prolonged use. Membranes with pore sizes of 0.2 to 2.5 µm would be an almost ideal solution for these problems if their stability and robustness did not set insurmountable limits to their use. [6], [7]

While there exist several patents for woven/non-woven coated filtration media for solid-liquid separation processes, only a few experimental results have been published on the subject. One of the few cases is Lydon's [24] study of three different versions of microporous low medium density polyurethane coating applied to a woven polyester multifilament fabric. His results suggest that the filtrate clarity, throughput and cake release of specifically designed media, combining multifilament substrate and microporous polyurethane coating, are clearly superior to those achieved with a conventional needlefelt filter media, both in vacuum and pressure filtration tests.

In a more recent publication, Lydon [25] also mentions another coated fabric based on spraying or knifing thermosetting resins for polypropylene and polyamide plain weave substrates, to give the filter fabric good abrasion resistance and dimensional stability. The abrasion resistance of resin-treated and untreated media were tested using a standard Martindale Abrasion tester equipped with SiC abrasive paper. Compared to the untreated medium, the resin-coated product can take roughly twice the number of abrasion cycles. Test filtration of kaolin slurry at 4 bar in a filter bomb indicated that, although the air permeabilities of the untreated fabrics were initially almost tenfold that of the treated, the filter throughputs were only marginally lower for the treated fabrics. Field trials with kaolin proved that the lifetime, cake discharge performance, and stretch resistance of the resin-treated substrate is superior to the respective virgin media.

Another recent case presented by Maurer [26] combines multifilament polypropylene filter fabric with a high abrasion-resistance and elastic polyurethane membrane. According to his test results, the offsets of the protective fabric protect the membrane in the fabric cavities. Abrasion of the tips during operation is inevitable but does not greatly impair the

performance. Test results obtained with china clay and titanium oxide (to the authors knowledge, one of the most demanding slurries) support Lydon's finding on being able to produce clearer filtrates and having good cake release while maintaining satisfactory permeability.

3 Clean media permeability and pore size

As stated by Tiller [2] “Nothing is more basic to cake filtration than porosity”. As shown by the basic equations below media permeability greatly depends on the porosity and tortuosity. This same notion also seems to hold for the particulate beds as shown by Paterson [40] and Dias in 2005 [41]. Unfortunately, porosity is only an aggregate measure of medium pore size and shape distribution, and as such does not always predict the particle capture capacity accurately enough.

3.1 Flow through particular beds

Septum or medium permeability is an overall measure of its resistance to fluid flow. Basic laws governing the flow of fluids through uniform incompressible beds have been utilised for developing modified formulae for various deep-bed and other media filtration applications. Darcy’s law is a generalised relationship for flow through porous media. It constitutes a definition of media permeability k for single-phase and one-dimensional laminar flow [3]. The Poiseuille equation expresses the viscous and laminar fluid flow through a single circular capillary, where $v = q/\varphi$ is the average velocity of fluid in the capillary and φ is the media porosity [2]. Thus, the Hagen-Poiseuille volume flow rate for laminar flow in circular pipes, where d is the diameter of capillary, n_p is the number of capillaries and l is the length of capillary, is: [39]

$$Q = -\frac{\pi n_p d^4}{128\mu}\frac{dp}{dx} = \frac{\pi n_p d^4}{128\mu}\frac{\Delta p}{l} \qquad (3.1.1)$$

The pores of a medium, however, are rarely sized or shaped exactly the same and at best only the pore size distribution is available from analysis. This presents a problem, as each different pore size would result in a unique value for pressure drop, and it would be practically impossible to calculate and sum up all the pore pressure drops to produce a comprehensive estimation of medium. To overcome this difficulty, various concepts like hydraulic radius and effective pore size have been introduced. These concepts usually

define one single pore size and shape to be representative of the multitude of pore sizes and shapes actually present in the medium. In other words, the pores are assumed to be identical in size and shape while the number of these pores is assumed to be the same as the true number of pores.

In cases where the pore cross-sectional area and wetted perimeter are known, the effective radius *r* has been defined as the hydraulic radius R_H that is, [3]

$$r = R_H = \frac{d}{4} = \frac{volume\ of\ void}{wetted\ surface} = \frac{void\ volume}{solid\ volume}\frac{volume\ of\ solids}{surface\ area} = \frac{\varphi}{1-\varphi}\frac{1}{S_0} \qquad (3.1.2)$$

where S_0 is the specific surface of the pore or fibres.

In most particulate beds, the actual fluid flow path *l* is longer than the bed thickness *L* and, consequently, the velocity along the path must be correspondingly greater than that for travel through the bed in a non-deviating direction perpendicular to the inlet and outlet faces. Introducing the tortuosity factor $\tau = l/L$, substituting the hydraulic radius (3.1.4) in the Poiseuille equation and integrating over the bed, yields

$$q = \frac{\varphi^3}{k_o \mu S_0^2 (1-\varphi)^2}\left(\frac{L}{l}\right)^2 \frac{\Delta p}{L} \qquad (3.1.3)$$

where $K = k_0 \tau^2$ is the Kozeny constant and k_0 is a factor which depends on the shape and size distribution of the cross-sectional areas of the capillaries. Assuming 45° of actual average flow direction for the longitudinal axis (τ^2 = 2), and an elliptical, rectangular or annular shape of capillaries ($k_0 \cong 2.5$), we arrive at the well known Kozeny-Carman (also known as Blake, Fair-Hatch) equation, which serves as a useful tool for illustrating the inter-relationship of the most important parameters. [3]

Paterson [40] proposed in 1983 that tortuosity can be incorporated in the hydraulic channel model (also called the equivalent channel model) to predict the permeability and electrical conductivity of fluid-saturated rock-bed. A formula similar to the Poiseuille equation was taken to apply to the equivalent channel, provided that the hydraulic radius R_H was taken

to be the characteristic cross-sectional dimension of the equivalent channel for determining the bulk flow rate, and another numerical constant *C* was taken to be the actual pore shape. The factor *C* was calculated for channels of simple uniform cross-sections, assuming the Navier-Stokes flow equations with non-slip conditions, giving *C* = 1/2 for circular cross-sections, 3/5 for equilateral triangular cross-sections, and 1/3 for a slot. The equivalent channel model gives the flow rate in the bulk flow direction

$$v = -CR_H^2 \varphi (\frac{L}{l})^2 \frac{1}{\mu} \frac{dp}{dx} \tag{3.1.4}$$

According to Paterson, there is an analogy for electrical conductivity measurement on the same rock saturated with an electrolyte solution. Application of Ohm's law gives

$$I_A = -\kappa_m \frac{dU}{dx} = -\frac{\kappa_m}{\kappa} \kappa \frac{dU}{dx} = -\frac{1}{\Omega} \kappa \frac{dU}{dx} \tag{3.1.5}$$

where I_A is the macroscopic current density in the direction of a coordinate *x*, *dU/dx* the macroscopic voltage gradient in the same direction, κ_m the electrical conductivity of the saturated porous medium, and κ the electrical conductivity of the fluid. The quantity Ω, the ratio of the electrical resistivity of the saturated porous medium to that of the fluid, is called the formation resistivity factor, and can be seen to be the tortuosity/porosity ratio that arose in connection with the equivalent channel model. As an analogy to the fluid case, it is assumed that all of the electrical current passes through the space of fluid-saturated pores, following paths that are identical to those followed by the fluid flow, and that the flow of electrical current can be represented in precisely the same way by an equivalent channel model as in equation. (3.1.6). Consequently, the total current passing through the medium is given by

$$I = I_A A = (\kappa \frac{\varphi AL}{l} \frac{L}{l})(-L \frac{dU}{dx}) \tag{3.1.6}$$

3.2 Permeability and open pore area of monofilament fabrics

In filtration, a woven fabric can be visualised as a network of capillaries having effective pore radius *r*, porosity *φ* and tortuosity τ, as shown by Bird *et al.* [43] as early as 1960. Metallic precision-woven fabrics (sometimes referred to as wire mesh or screens) are probably the closest woven structures to an ideal situation, when it comes to being able to use simple orthogonal procedure to estimate the area of each mesh spacing. For a metallic network, Bruncher proposed a hydraulic radius, equation (3.1.2), that is consistent with Bird *et al.* classical definition of porous media. [44]

For example, Brundrett [45] has used the well-known works of Pinker and Herbert (1967), Schubert *et al.* (1948), Tan-achitat *et al.* (1982), Groth and Johansson (1988) and Munson (1988) to develop a prediction model of pressure-drop for metallic wire mesh. Although Pinker and Herbert noted that the effective open area of a screen must be somewhat greater than that obtained from simple orthogonal subtraction of the wire blockage from the area of each spacing, they used the following geometrical formula to estimate the screen porosity,

$$A_o = (1 - s_1 d_1)(1 - s_2 d_2) \qquad (3.2.1)$$

which is identical to the cover factor equation (2.1.4.). Pinkert and Herbert proposed that the pressure drop coefficient K_0 defined for incompressible flow perpendicular to the screen, in terms of the screen pressure drop and upstream velocity is

$$\Delta p = K_0 0.5 \rho v^2 \qquad (3.2.2)$$

They concluded that K_0 could be separated into two independent components, a screen open area function $G(A_o)$ and a function based on the wire Reynolds number f(Re_d) ($Re_d = vd/\eta$).

Pederson [3] adopted an orifice analogy to interpret flow-pressure loss behaviour for monofilament media with various weave patterns. He related the basic variables (warp and weft setts, warp and weft diameters and weave) of a fabric to the effective area of orifice

A_e and wetted orifice perimeter W. He proposed that the flow through textile media can be treated as a flow through narrowing and subsequently widening flow channels, and a discharge coefficient for laminar flow was formulated as

$$C_D = \sqrt{\frac{\rho v^2}{2\Delta p}\frac{(1-A_o{}^2)}{A_o^2}} \tag{3.2.4}$$

where

$$A_o = A_e s_1 s_2 \tag{3.2.5}$$

Pederson used experimental air permeability data on plain and 2/2 twill fabrics to verify the discharge equation (3.2.4), and obtained a good correlation between the discharge coefficient and the air Reynolds number, with an average error of about 12 %.

The effective open areas of symmetrical monofilament weaves like 1/1 plain weave and 2/2 twill weaves are easy to define as proposed by Pederson and later on by Lu *et al.* [44], because, in these cases, the fabrics are made up entirely of identical pores. Rushton *et al.* [46] also used water to develop the discharge coefficient as a function of Reynolds number for plain, twill, and also 5/1 satin weaves. For plain and twill weaves, they propose the following empirical correlation with a maximum error of 18 %

$$C_D = 0.17(\mathrm{Re})^{0.41} \qquad 1 < \mathrm{Re} < 10 \tag{3.2.6}$$

where

$$\mathrm{Re} = \frac{4\rho v}{W s_1 s_2 \mu} \tag{3.2.7}$$

The situation becomes more complicated in the cases of other types of yarns and weaves as a multitude of pores types occur side by side, and sometimes on top of each other (multiple layered weaves). An effort to correlate the 2/1 twill with 5/1 satin weave led Rushton *et al.* to the definition of “flow cell”, which is a repeated pattern in the cloth. To calculate one single value for the effective fractional open area and wetted perimeter of the

pore, they used a fractional weighting procedure based on the number of plain and twill pores present in the flow cell.

3.3 Permeability, effective pore size and open area of multifilament fabrics

Ripperger *et al.* [47] propose that the Darcy equation, as follows, can be used to determine the effective pore size of a multifilament woven fabric, provided that the measured permeability, porosity and pressure drop data are available:

$$d_{p,eff} = \sqrt{\frac{32K}{\varphi}} = \sqrt{\frac{32vL\mu}{\varphi\Delta p}} \qquad (3.3.1)$$

Unfortunately they do not present experimental results comparing the measured and calculated effective pore sizes.

Takada *et al.* [48] studied the air permeability of woven and knitted spun yarn fabrics in relation to porosity. Their experimental results were analysed according to the Kozeny-Carman equation. Assuming circular flow channels, using the density porosity and media-specific surface calculations, they determined the fabric-specific permeability and pore area coefficient using the Kozeny-Carman equation. Although specific correlations are not given in the publication, it is claimed that the results support the prediction of specific permeability and pore-area coefficient over a wide range of permeabilities.

As reviewed by Brasquet and Cloirec in 2000 [42], the literature contains fairly little information about the fluid pressure drops through multifilament woven fabrics, apart from Goodings (1964), which enables a fabric-opening diameter to be calculated from air pressure drop measurements, or Belkami and Broadbent (1999) which add a deflection term to viscous and inertial terms and to model pressure drops.

Firstly, Brasquet and Cloirec measured the air and water pressure drops induced by 20 different rayon and activated carbon woven cloths as a function of fluid velocity. Secondly,

they used straightforward regression analysis to find out the kinetic and viscous energy loss coefficients, *M* and *N* respectively, of the generalised flow equation (Reynolds, 1900)

$$\frac{\Delta p}{L} = Nv + Mv^2 \qquad (3.3.2)$$

Then they determined the fabric opening radii and opening specific surface using Gooding's relation.

$$\Delta p = \frac{8 l_0 \mu A}{\pi r^4 N_0} v + \frac{1.3 \rho A^2}{\pi r^4 N_0^2} v^2 \qquad (3.3.3)$$

In their study they used the measured cloth thickness *L*, specific planar weight *w*, and the number of warp and weft yarns per unit area to calculate the fibre length ($l_0 = L/2$), media density ($\rho_p = w/L$), external surface area ($S_f = 1/L$), porosity ($\varphi = 1 - \rho_p/\rho_f$) and number of openings per unit area ($N_0 = s_1 s_2$). *A* is the medium cross-sectional area. Taking the *N* value from the regression analysis of the equation (3.3.2) and solving for the effective pore diameter yields,

$$d_{p,eff} = 2\sqrt{\frac{4LA\mu}{\pi N N_0}} \qquad (3.3.4)$$

With these parameters they tested the suitability of classical models (Ergun, Carman dimensionless model and Comiti-Renaud) to describe the flow through woven structures. Belkacemi's model was not used because it was time-consuming for calculations, and one of the parameters, the angle between two crossed fibres, was not available. As a conclusion they found that none of the above classical models are suitable to describe the flow through the tested woven structures, and that the best way to model the pressure drop through woven fabrics is to use a statistical approach and neural networks to find out the highly interrelated correlations between specific characteristics of woven structures. A variable analysis confirms that the fabric characteristics, especially external surface area and number of openings per unit area, have the greatest influence on pressure drops.

Militky *et al.*'s [13] results confirm that the conventional orthogonal open area calculations do not allow for accurate porosity and permeability predictions with fabrics woven from stable fibre yarns. They tested 40 different types of wool, wool/polyester, polyamide and viscose woven fabrics for air permeability, light transmission and three different conventional idealised porosity calculations. The first calculation was based on the density porosity presented in equation (2.1.4).

The second was based on the definition of a hydraulic pore for filtration purposes (Robertson, 1950),

$$\varphi_{Hw} = 1 - \frac{1}{L}\left[s_1 \frac{(1 + S_1/100)T_1}{525\ 10^3 \rho_{1f}} + s_2 \frac{(1 + S_1/100)T_2}{525\ 10^3 \rho_{2f}} \right] \qquad (3.3.5)$$

where S_1 and S_2 are the yarn-shortening percentages in the weft and warp due to crimping, and T_1 and T_2 are the linear densities of weft and warp yarn, respectively. The third evaluation was based on the classical Pierce definition of fabric cover factor, which leads to the pure geometrical presentation of the open area in equation (2.1.3).

They concluded that while the measured air permeability *AP* and media porosity φ evaluated from the light transmission images can be correlated fairly well (correlation coefficient R=0.85) using standard regression analysis as,

$$AP = 2.8881 \cdot 10^2 + 3.6364 \cdot 10^3 \varphi \quad \left[m^3 m^{-2} s^{-1} \right] \qquad (3.3.6)$$

the porosities computed from the geometrical characteristics of fabrics are far from how they are in reality.

As concluded by Dubrovski *et al.* [54], there is also a big difference between the macroscopic pores of fabrics made out of staple yarns, monofilament, or multifilament yarns. They measured the stereomicroscopic images of 27 woven plain, twill and satin fabrics. From these images, they determined the pore cross-section, pore density, and minimum and maximum (Feret's) pore widths of a pore. From these measurements they calculated two more macroporosity properties, namely open porosity and equivalent

circular pore diameter. They then used a least square optimisation technique to find the correlation between the independent variables, yarn fineness, weave value, fabric thickness, and denting (number of yarns per reed dent) and their dependent variables. The dependent output variables were area of pore cross-section, maximum pore diameter, minimum pore diameter and pore density (number of pores per cross-sectional area).

They concluded that it is almost impossible to observe all fabric types to predict macroporosity, not to mention the inter-yarn microporosity. They have focused their investigation on cotton fabrics made from stable yarns. For the type of fabrics used in the model derivation, the deviation between predicted and measured values is below 5 % but for random cotton stable yarn fabrics, the deviation is about 10 %. For other types of fabrics and raw materials, there is no data available.

As discussed by Rushton *et al.* [46] and several other authors as early as the 1980's, densely woven multifilament fabrics contain both intra-yarn and inter-yarn pores, which both contribute to the fluid flow. The ratio of a multifilament or staple fibre cloth overall permeability k to the permeability of a similar monofilament cloth k_m,

$$\beta = \frac{k}{k_m} \tag{3.3.7}$$

has been shown to vary in the range of 1 to 20, the high-end values correlating to low overall permeabilities. [7]

The problem of prediction of overall permeability, using easily measured cloth properties such as cloth, yarn and fibre densities, has not yet been completely resolved. If it were possible to evaluate the specific permeability of the yarns k_y, in situ, without removal from the fabric, Wakeman and Tarleton [3] suggest Brinkman's approximate solution to calculate the β ratio

$$\beta = \left(1 + 1.80\frac{k_y}{k_m} + 2.68\sqrt{k_y / k_m} \right) \quad \text{for} \quad \frac{k_y}{d_y^2} < 0.0017 \tag{3.3.8}$$

The technique of stripping a yarn and calculating the yarn density from the weight of a measured length of yarn, however, produces quite serious errors in those cases where yarn compression effects are large, such as in tightly woven multifilament fabrics. These difficulties result in the recorded value of the yarn density being less than the cloth bulk density. Therefore, in the multifilament cloth cases, Rushton proposes that, for low β factor cloths of plain weave, the following monofilament equation may be used:

$$k = \frac{d_y^2}{(1-\varphi)^{1.5}\left[1+56(1-\varphi)^3\right]} \qquad (3.3.9)$$

For tightly woven cloths of high β factor, however, the equation below has been suggested. Here the characteristic fibre dimension d_f is used since most of the flow occurs over the fibres:

$$k = \frac{d_f^2 \cdot 10^{-5}}{2(1-\varphi)^{6.5}} \qquad \beta > 16 \qquad (3.3.10)$$

For the intermediate range $1.2 < \beta < 10$, the equation below has been produced from the cloths studied up to the present:

$$\log \beta = 0.0234 + 0.0408 \frac{(\rho_f - \rho_y)}{(\rho_y - \rho_p)} \qquad (3.3.11)$$

In addition to the standardised air permeability measurements like Frasier Low Pressure Machine or Gurley Densometer, and the consecutive pore size calculations, there exist two alternative methods for determining the open pore size distribution of media as reviewed by Rideal *et al.* [49].

The bubble point measurement is based on the Washburn equation which he derived from the Hagen-Poiseuille model via Laplace transform. Firstly, the sample cloth is wetted thoroughly with all of its pores filled with liquid. For tightly woven multifilament fabrics, it is sometimes necessary to use vacuum impregnation so as to eliminate any occluded pockets of air. For the determination of the bubble point, the air pressure is slowly increased whilst observing the surface of the liquid and the sample. According to the

Washburn equation, the equivalent pore diameter d (assumed to be cylindrical again) corresponding to the liquid film break-through-pressure of the medium surface (the first air bubbles detected coming thought the media) p, is dependent on the contact angle θ between the liquid and the pore wall and the surface tension of liquid σ. For the desired test liquids which are fully wetting, the contact angle is zero, so the equation simplifies to:

$$d = \frac{4\sigma}{p} \qquad (3.3.12)$$

As the pressure is further incrementally increased, general bubbling develops, the air flow increases accordingly and finally all the test liquid bursts out of the pores of the medium.

Today, the technique to measure the medium pore size distribution automatically using liquid extrusion and capillary flow porometers is well-established, mainly by Porous Materials Inc. (PMI) and Coulter. This procedure involves conducting a wet run and a dry run on the same sample, while the readings of flow rate versus pressure are logged at frequent intervals. The point at which the wet run curve leaves the base line corresponds to the bubble point pressure from which the maximum media pore diameter is calculated using the equation (3.3.8). Similarly, the point where the wet run and dry run plots converge corresponds to the minimum pore diameter. Superimposing an extra “half of dry run” plot on the data identifies the mean flow pore diameter at the intersection of the half dry curve and the wet run curve.

The automation of both the Coulter and PMI instruments has made the old ASTM F316 method obsolete, and brought porometry into general use by most media manufacturers. As shown by Gupta and Jena in one of their several publications on porometer use [50], [51], [52], the technique has proven to be versatile and especially suitable for the analysis of non-woven filter media.

Epps and Leonas [11] used the liquid extrusion method that forms the basis of the ASTM Test Method E 1294-89 to study ten different woven fabrics for correlation between measured air permeability (ASTM D737), porosity (ASTM E1294), mean flow pore size, minimum pore size, maximum pore size and calculated porosity and cover factor. Based on their findings, the highest correlation among the studied variables was a correlation

coefficient of 0.9264 between air permeability and minimum pore size. Air permeability was also significantly correlated with the mean flow pore size, but not with maximum pore size. The calculated percentage of porosity also significantly correlated with the mean flow pore size, and minimum pore size, but not with maximum pore size.

As shown by Mayer [53] the primary limitation of the liquid extrusion porometry lies in the theoretical basis of symmetrical cylindrical straight pores, very unlikely to occur in woven multifilament and stable fibre fabrics. A second limitation of the method may be a lack of precision in measurements of thick or irregularly textured fabrics. A third limitation is that the method relies on fluid transport, dependent upon complete wetting of the specimen and subsequent complete evacuation of the fluid, which may be difficult to achieve in hygroscopic textile fabrics.

The general form of the Purcell equation gives empirical evaluation for permeability by the equation of capillary pressure of mercury injection *p*,

$$k = \frac{(\sigma \cos\theta)^2}{2} \varphi \sum \frac{S_{Perc}}{p^2} \qquad (3.3.13)$$

where S_{perc} is the percentage of mercury saturation. The commercial method, called mercury porosimetry or mercury intrusion porosimetry, involves filling the pores with mercury under high pressure. The volume of the mercury forced in, which can be measured very accurately, is related to the pore size and the pressure. From the filter media manufacturer's point of view, the main drawbacks of the method are the inherent inability to differentiate between dead-end pores and pass-through pores, and the high pressures involved.

Recent advancements in the challenge test method, in which particles of known size distribution are presented to a filter, and any changes downstream are measured by a particle size analyser, are making it possible to achieve higher absolute accuracy in medium pore size distribution measurements in the range of 20 to 200 μm [55]. The improved method using glass microspheres of narrow particle size distribution was produced using highly accurate electro-formed sieves instead of conventional, irregularly-shaped test dust. To ensure the transportation of the microspheres through the tortuous

path in the complex filter structure, a Sonic sifting device is used to fluidise the microspheres rather than shake the filter. According to Rideal *et al.* [49], the comparative results of the new challenge test show good agreement between porometer measurements and the new method.

4 Cake filtration and the medium resistance

As stated by Mayer [1] in one of his numerous publications on cake filtration, cake filtration predominates both in the usual separation devices such as nutsches, centrifuges, vacuum filters, belt filters, and filter presses and also in automatic vacuum pressure filters, thickeners, candle filters and filter aid filters, and, in some instances, cartridge filters.

4.1 Cake Filtration theories

As reviewed for example by Oja [56], it is convenient to use the Ruth modification of the Darcy equation (3.1.1) as the starting point for most experiments in cake filtration

$$\frac{dp_L}{dw_m} = \mu\alpha q + \mu R_m \qquad (4.1.1)$$

where w_m is the mass of dry solids deposited per unit area, R_m is the medium resistance and α is the specific cake filtration resistance. Relating the Kozeny-Carman equation to the Ruth equation (4.1.1) and assuming negligible medium resistance, it is possible to show that the specific resistance of a cake is related to permeability and specific surface:

$$\alpha = K\frac{(1-\varphi_c)}{\rho_s\varphi_c^3}S_o^2 \qquad (4.1.2)$$

In practice most cakes are compressible to a certain degree and their specific resistance changes with the pressure drop Δp_c across the cake. In such cases, an average specific cake resistance α_{av} can be used in equation (4.1.1.)

$$\frac{1}{\alpha_{av}} = \frac{1}{\Delta p_c}\int_0^{\Delta p_c}\frac{d(\Delta p_c)}{\alpha} \qquad (4.1.3)$$

Replacing dp_L by compressive pressure over the solid cake dp_s, rewriting the equation (4.1.1) and integrating over the entire cake from the beginning of the filtration (p = 0) until the end of the filtration ($p = p\text{-}p_1$), where $p_1 = \mu q\, R_m$ is the pressure required to overcome the resistance of the clean medium R_m, yields the following basic approach to constant pressure, constant rate, and variable pressure-variable rate types of filtration operations:

$$\mu qcV / A = \int_0^{p-p_1} \frac{dp_s}{\alpha_{av}} = \frac{p - \mu q R_m}{\alpha_{av}} \qquad (4.1.4)$$

This equation has been presented in many forms (Sperry 1916, Grace 1953, Heertjes 1975, Purchas 1981, Svarovsky 1983, Willis 1983), of which the general resistance form (Leu and Tiller 1983) is

$$q = \frac{1}{A}\frac{dV}{dt} = \frac{p}{\mu(\alpha_{av} w + R_m)} \qquad (4.1.5)$$

By assuming that the solids concentration, the average specific filtration resistance and the medium resistance are constant (that is to say, obtain their final value immediately), the general equation can be conveniently written for constant pressure filtration test result interpretation as

$$\frac{(t - t_s)}{(V - V_s)} = \frac{\mu c \alpha_{av}}{2A^2 \Delta p}(V + V_s) + \frac{\mu R_{mf}}{A \Delta p} \qquad (4.1.6)$$

where t_s is the time before the constant filtration pressure, V_s is the volume of filtrate collected during this period, and R_{mf} is apparent medium resistance. R_{mf} consists of two components: the true (or clean) medium resistance and the resistance of the filter cake layers collected on and in clean media before the time t_s . According to Grace, the equation (4.1.9) can be used, if the apparent medium resistance is less than 10 % of the total resistance and if the filtration lasts for more than just a few minutes.

For constant rate filtration, q is constant and the equation (4.1.6) can be written

$$p - \mu q R_m = c\mu\alpha_{av} q^2 t \qquad (4.1.7)$$

4.2 Compressive cake filtration and porosity

For incompressible filtration, the cake solids concentration (alternatively porosity or solidosity) and permeability would all be constants under conditions of constant pressure, resulting in linear correlation with the hydraulic pressure gradient along the cake height. In practice, however, this is rarely the case, as demonstrated by the studies of Fathi-Najafi and Theliander [57], Johansson and Theliander [58] for several mineral slurries, and Ingmanson and Whitney [59] for various pulp slurries. They suggest that the Kozeny-Carman equation can be used only if the functional relationship between the solids concentration in different layers inside the cake (or porosity), respective specific resistance and the local compressive pressure are known.

It is generally assumed in compressible cake theory that the local porosity and specific filtration resistance are unique power functions of the drag or solid compressive pressure $p_{s.}$. For example Grace (1953) and Tiller (1955) [38] used the compression-permeability (C-P) cell developed originally by Ruth to study the compressibility in cake filtration. In using the C-P model, it is assumed that the cake porosity and specific resistance are unique functions of the applied mechanical pressure by piston. In interpreting the C-P cell results it is further assumed that the frictional drag pressure is equal to the mechanically applied pressure, and the porosity and alpha of identical cakes in a filter press and a C-P cell are identical.

As discussed, for example, by Wakeman [61], the principal inaccuracies of C-P cell testing result from side-wall friction, the time lag required to reach an equilibrium porosity, the change of cake characteristics with time and the inability of a C-P test to reveal concentration effects. Wakeman used Darcy's law as a starting point to develop a comprehensive mathematical-physical analysis of the kinetics of cake filtration. He recognised cake filtration as a moving boundary problem and utilised a variable compressibility coefficient in the form of an exponential function of porosity. In his analysis,

he was able to show that the pressure distribution and porosity profiles inside the cake vary significantly, and that both the porosity and specific resistance vary with filtration pressure and solids feed concentration.

The problem with finding out the empirical parameters for the compressibility and permeability using the C-P cell and other constant pressure filtration mode tests, is that the characterisation time is very high. Standard constant pressure filtration requires five or more individual filtration tests to characterise a suspension across a range of solids concentrations. To shorten the testing time, de Kretser *et al.* [69] have developed the stepped pressure compressibility filtration test. This test requires just one complete stepped pressure compressibility filtration test and one truncated stepped pressure permeability filtration test using the fundamental theory of Landman *et al.* [70] to determine the hindered settling function $R(\varphi)$ and compressive yield stress $P_y(\varphi)$. For the stepped pressure regime of the test, however, the amount of data available within each constant pressure phase is more restricted, and so, potentially, is the accuracy of the data manipulation, unless sophisticated, mechatronic-based testing equipment with a high degree of automation is available [71].

Johansson and Theliander [58] used gamma-ray attenuation to obtain the concentration and pressure profile of a lignin filter cake simultaneously. At a constant filtration pressure of 1.1 MPa, the lignin cake solidosity gradually develops in time, starting from the medium surface and finally reaching the top of the cake. Similarly, the solid compressive pressure is zero at the start but, as the cake builds up and the solidosity increases, p_s increases due to drag forces. This large pressure drop close to the medium is typical of compressible filter cakes, being caused by the skin effect.

As suggested already in 1953 by Rietema, it is possible that a so-called “retarded packing compressibility” (RPC), where parts of the forming filter cake appear abruptly to change structure and collapse, can take place during the filtration. In 2001, Tarleton *et al.* [62] showed that, during the cake build-up, a measured reduction in the cake solids concentration part way through a filtration, was accompanied by an increase in filtrate flow.

4.3 Conditions for pore bridging and the role of filter media

As already discussed in chapter 1, the role of filter media is probably most important in the early stages of cake filtration when the first solid particles arrive on the surface of the media. Proper cake filtration conditions are created only when the pores of the media are sized and shaped so that the arriving particles can form sufficiently strong and stable bridges across the pores. As reviewed by Rushton *et al.*[9], Hixson *et al.* used sand slurries and glass capillary tubes immersed in highly concentrated quartz suspensions, and reported the relationship below pore diameter and mean particle size d_p for bridging concentrated suspension (solids concentration higher than 20 % w/w):

$$d = K_1 (d_p)^{1/4} \quad \text{where} \quad K_1 = 175\, m^{3/4} \text{ for Hixson's data} \qquad (4.3.1)$$

Recent work by Rushton *et al.* [46] has demonstrated that the K_1 value depends on the structure of the particle and varies from 175 $m^{3/4}$ up to 500 $m^{3/4}$. It may be seen that as the particle becomes more 'sand-like' in composition the value decreases. They derived an empirical relationship between the slurry concentration, mean particle size and open pore size,

$$d = K_2 d_p c^m \quad \text{for} \quad c < 20 \ \% w/w \qquad (4.3.2)$$

for capillaries and for various plain weave monofilament cloths, using a particle concentration range 0.002 % w/w < c < 2 % w/w in the latter case and 2 % w/w < c < 30 % w/w for capillaries. Typical values for the K_2 range were 10.2 – 20.8 and for m 0.26 – 1.04. They conclude that the data available at present is insufficient to provide a relationship for pore types other than plain type pores, and the situation is aggravated further in the case of multifilament cloths since, in addition to the uncertainties associated with possible flow division, cloths of stable fibre must be considered along with continuous filament yarns. Much more controlled experimentation is required in this complex field before a complete explanation of cloth effects can be postulated.

For example, Smith and Maroudas and Eisenklam state the filter cake cannot form below a certain critical feed concentration, as the particles arrive individually and cannot form a

stable bridge. Similarly, if the applied pressure is above a certain critical value or the interstitial velocity exceeds a certain value, particles cannot form a stable bridge. In general, the probability of particles bridging a pore will depend upon many factors, including particle concentration, particle-to-pore-size ratio, size spread and skewness of the impinging cloud, pore shape and cloth type, be it monofilament or multifilament. [8]

In a recent work by Lu *et al.* [8], the flow field and pressure drop of fluid flow through the four basic pore structures of the most common weaves of filter cloths, namely plain, twill and satin, were studied numerically by numerically solving the equation of continuity and equation of motion where all space-variable and flow quantities are normalised with respect to the equivalent pore diameter, D_e, and approach velocity, u, far from the inlet of the filter pore.

Rainer and Höflinger [63] used computational fluid dynamics to study the different stages of the cake building process of two media types, namely Dutch weave and slotted metal sheet. They used a diatomite test suspension to allow microscopic visualisation of the different stages of the cake build-up, overall pressure drop of the filter media and its interaction with the primary cake layer, fluid flow, turbidity of the filtrate or the number of particles in the filtrate to be recorded and evaluated over time.

4.4 Flux of ions through a diaphragm fabric

In the nickel electrowinning processes, nickel is precipitated from a nickel sulfate solution into metallic form by electric current. The desired cathodic reaction is the reduction of nickel ions on the cathode plate, and the main anodic reaction is the decomposition of water on the surface of the lead anode. Simplified cell reactions can be described by the following overall reactions. [66]

Cathode reactions:	$Ni^{2+} + 2e^- = Ni$	$E^o = -0.23$ V
	$2H^+ + 2e^- \rightarrow H_2$	$E^o = 0.00$ V
Anode reaction:	$H_2O = 2H^+ + ½\ O_2 + 2e^-$	$E^o = 1.229$ V

Cell reaction: $NiSO_4 + H_2O = Ni + H_2SO_4 + ½ O_2$

As explained in more detail in publication in Appendix VII, industrial scale nickel electrowinning operations around the world use tightly woven diaphragm fabrics to enhance the quality and quantity of nickel production. The diaphragm cloth resists the electrolyte flow from the cathode compartment to the anode compartment and, by doing so, forces the electrolyte to accumulate in to the cathode compartment until the liquid level is high enough to overcome the fabric flow resistance. As discussed in the previous chapters the permeability of a woven fabric is proportional to the fabric thickness, tortuosity and pore structure (the size, shape and number of pores).

Ions in an electrolyte can move between the catholyte and anolyte by means of diffusion, migration and convection. The higher the electrolyte feed flow and the resulting flow through the fabric, the higher the convective mass transfer. Similarly, the higher the concentration difference between the anode and cathode compartment, the higher the diffusive mass transfer, other things being the same. Without a diaphragm fabric, the back-diffusion off acid is significant and the optimal reduction pH can not be maintained.

Mass transfer to an electrode is modelled by the Nernst-Planck equation. As presented by Lenthall *et al.* [67], the equation (4.4.1) can be used to model the net flux of species *i* through a porous diaphragm, due to migration, diffusion and convection:

$$j_i = vA_0 c_i(x) - \frac{IFD_i z_i c_i(x)}{RH\kappa} - D_i A_0 \frac{dc_i(x)}{dx} \qquad (4.4.1)$$

When integrated between the boundary conditions $c_i(0) = c_c$ (catholyte concentration) and $c_i(d) = c_a$ (anolyte concentration), the following equation for the flux of species *i* through the diaphragm is yielded,

$$j_i = -\xi_i D_i \frac{\left(c_{i,a} - c_{i,c} \exp\left(\frac{-\alpha_i d}{A_0 \varphi} \right) \right)}{1 - \exp\left(\frac{-\alpha_i d}{A_0 \varphi} \right)}$$

where (4.4.2)

$$\xi_i = \frac{IFz_i}{RH\kappa} - \frac{vA_0}{D_i}$$

and *F* is the Faraday constant, *H* is the temperature, *I* is the current, and D_i is the diffusion coefficient of species *i*.

In order to be able to use equation (4.4.1) for diaphragm mass transfer simulations one would have to have accurate values for diffusivity of each ionic species and all combinations in the system and the average conductivity of the solution κ in the diaphragm. As shown by Awakura *et al.* [64], the diffusivity of $NiSO_4$-H_2SO_4 solution depends on the concentration of both the acid and the salt. Similarly the conductivity of the solution is dependant on the concentration of the solution in the diaphragm.

5 Experimental methods, results and discussion

5.1 Problem description and motivation for the thesis

The motivation for developing calendering, coating or a chemical treatment for existing woven liquid filtration media was to enhance the small-size particle capture in pressure filtration, to ensure good dirt-repellancy in de-inked pulp dewatering and to reduce the energy consumption in the nickel electrowinning process.

The present plain woven cloths used in the above applications are the result of almost century-long field trials with numerous testing of different combinations of yarn and weave types. Consequently, it is becoming increasingly difficult to improve the present designs simply by altering the yarn or weave types.

On the other hand, up to now, there have been only a few successful attempts to coat or treat woven media to produce commercially-viable products, as discussed in section 2.2 of the literature survey. The first challenge in developing a coating or chemical treatment for woven medium is the inevitable reduction in open area, resulting in lower permeability and subsequent loss of deliquoring capacity, due to the treatment. This means that the woven fabric structure has to be altered to have a somewhat higher open area than the respective plain cloth. If the applied treatment, however, is not able to compensate for the loss of mechanical strength, the treated product will have inferior mechanical properties.

Another, and usually a much more significant, complication is the adherence of the treatment to the substrate. Polymeric yarns in a woven structure are abrasion-resistant, and, for decades, multifilament fabrics in particular have been used successfully in highly abrasive mineral applications. Even after having lost as much as 10-20 % of its original mass, a plain multifilament cloth may still work without any significant reduction in any of its important performance characteristics. Coatings and treatments, on the other hand, are by definition present only on the surface of the yarns or media as relatively thin films, and thus they are prone to abrasion in a much more significant manner.

A third obstacle to the widespread use of coatings and treatments is the additional cost involved in applying the treatment. In most cases special equipment and additional raw-materials are needed to realise the treatment. Due to the relatively low cost of PET and PP yarns, the potential savings in manufacturing somewhat lighter substrate fabric for the treatment are easily offset by the high investment costs and expensive raw materials involved in realising the treatments.

For most filtration cloth manufacturers, the product line has to be broad enough to cover several different sizes, mechanical strength, open area and particle capture. In order for the coating and chemical treatment process to be economical, it should be versatile enough to allow treatment of several different kinds of fabrics, ranging at least from simple monofilament fabrics to more heavy multifilament and spun yarn fabrics.

The main aim of this work was to develop and test various coatings and treatments for the most common woven media used in selected liquid filtration applications. The performance of the coated or chemically and thermally treated media was compared to the respective woven cloth performance used in laboratory-scale filtration tests.

For de-inked pulp dewatering applications, the commercially available dirt-repellent chemical treatments and specially blended yarns were tested in order to verify their effectiveness vis-à-vis the non-treated cloths.

For the filtration of PCC slurry, several coatings and treatments were developed and tested both in constant rate and stepped pressure filtration modes, as opposed to the plain woven media performance.

Finally a new method of applying polyaniline coating on top of a standard multifilament cloth for nickel electrowinning process was developed and tested in terms of process performance, including standard weathering testing.

In section 4 of the literature survey, the theories investigated to understand the correlation between the media pore size and open area for cake filtration performance are presented. Reviewed in section 3 are several theories and methods to measure the pore size and open area of woven fabrics. As explained in section 3 most of the developed methods

require the use of special equipment and measurements in order to predict the pore sizes and open area of woven cloths. The results presented by the authors also indicate that the problem of being able to estimate the pore size and open area is still partly unsolved.

The idea of being able to measure changes in the effective pore size of liquid filtration cloths arose when the chemical treatments and coatings and their effect on electrical resistance and permeabilities were measured hundreds and hundreds of times. The correlation between the electrical resistance and permeability of media proved to be highly ambiguous, and this sparked the idea of first theoretically using the theories presented in section 3 of the literature survey, and, later on, empirically studying the possibility of using both these measurements to produce a more accurate value for the effective pore size and open area of a woven cloth. This work resulted in a new method of estimating the effective pore size and open pore area in a densely woven multifilament fabric. The results are validated by comparing them to the measured values of the largest pore size (Bubble point) and the average pore size using an industrial porometer.

5.2 Woven fabrics used for this study

Standard woven and heat-stabilised fabrics by Tamfelt Corporation used to study the coatings and chemical treatments developed in this study are listed in table 5.2.1.

Table 5.2.1. Standard woven media used in the study.

Weave	**Warp yarn**	**Weft yarn**	**planar weight, gm^{-2}**	**Air permeability, $m^3m^{-2}s^{-1}$**	**Used in the following studies**
Plain	PET multifilament	PET multifilament	560	0.5	Appendix I, III, V, VI and VII
Plain	PET multifilament	PET spun yarn	380	0.6	Appendix III
Plain	PP multifilament	PP multifilament	315	0.9	Appendix II
Satin	PP multifilament	PP spun yarn	560	1.6	Appendix II, III
Twill	PP multifilament	PP multifilament	330	25.0	Appendix II
Twill	PET spun yarn	PET spun yarn	490	2.0	Appendix II
Twill	PP monofilament	PP monofilament	200	265.0	Appendix II, IV

The above basic fabrics are the result of decades-long development work in full-scale process use, and form a solid reference base for the development of innovative coatings and chemical treatments for the specified applications. In this work, they were also used as the starting point in the weaving of suitable base fabrics for the coatings and treatments by altering their structure as little as possible.

5.3 Analytical methods for testing fabric properties

For the papers presented in appendices I to VII, selected single layer PET and PP and their respective coated or chemically-treated fabrics, all produced by Tamfelt Corp.'s Tampere factory, were manufactured. The loomstate fabrics were heat-stabilised and part of the heat-stabilised fabrics were subsequently calendered on the top-side. A portion of the top-calendered fabrics were further calendered on the bottom-side to a desired level of permeability. Coatings and chemical treatments were applied on both the heat-stabilised and calendered fabrics, depending on the application.

For each test fabric, the area mass, thickness, warp and weft density, air permeability, water permeability, porosity and specific electrical resistance were measured.

The following is a list of standards used to analyse fabric properties.

- Mass per unit area: SFS 3192 Textiles. Determination of mass per unit area and per unit length of textile fabrics.
- Thickness: SFS 3380 Textiles. Determination of thickness of textile fabrics.
- Warp and weft density: SFS 2984 Determination of number of yarns in woven fabrics (warp and weft densities).
- Air permeability: ISO 9237 Textiles. Determination of permeability of fabric to air (at 200 Pa).

The bubble point pore size and the average pore size were measured with the Porometer CFP-1100-AEX manufactured by Porous Materials Inc.. The tortuosity factor used throughout these measurements and calculations was 1.4, as recommended by Gupta *et al.*. [50], [51], [52]

Water permeability was measured with Tamfelt's industrial VLM-100 analyser. The pressure difference used in all water permeability measurements was 1,471 Pa (150 mm water gauge).

Dirt-repellence properties were tested with special testing equipment developed originally by UPM-Kymmene Research Centre. The test is based on placing the medium to be tested in contact with a pre-determined waste-paper slurry for 30 minutes in 55 ^{o}C, and then counting the number of attached particles through a microscope. In the calculation of the dirt-repellence index for the tested medium, the reference point was taken to be the number of stickies and dirt found on the reference fabric. The dirt-repellence index is calculated simply by dividing the number of stickies and other dirt particles found attached to the medium to be tested by the number of stickies and dirt found on the reference fabric.

The electrical resistance of the fabric was measured according to Tamfelt's own in-house standard in ambient air and with 10 w-% NaCl-solution. The analyser comprises a signal generator, an amplifier, a voltmeter, an ammeter and two electrodes. Alternating current, with a frequency of 4,000 Hz was used in the measurements.

The electrical resistance Ω_m through the fabric is simply calculated from the measured total cell voltage U_c with the fabric, and the cell voltage U_0 without the fabric, and I_c and I_0 are the respective currents.

$$\Omega_m = \frac{U_c}{I_c} - \frac{U_0}{I_0} \qquad (5.1.1)$$

5.4 Development of a novel technique for the estimation of fabric effective pore size and open area (Paper in appendix 1)

As presented, for example, by Paterson [42], the cross-section of a woven fabric can be considered to have a solid polymer layer and a solution-filled open pore layer as presented in figure. 5.4.1.

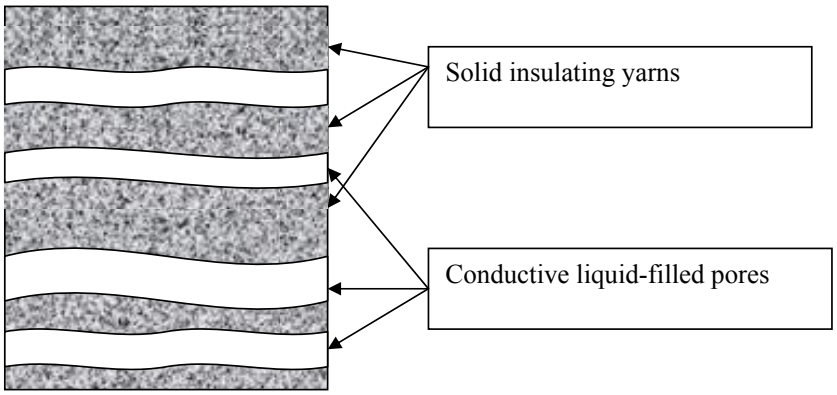

Figure.5.4.1. A schematic cross-section of the test fabric

Consequently, the overall electrical resistance through the fabric can be written as a sum of the resistances of the two substances

$$\frac{1}{\Omega_m} = \frac{1}{\Omega_y} + \frac{1}{\Omega_p} \qquad (5.4.1)$$

As shown by the author in Appendix I, it is possible to estimate the fractional open area of the pores from the measured electrical resistance

$$A_o \approx \frac{L\tau}{\Omega_m \kappa A} \qquad (5.4.2)$$

In addition, by using the estimated total open area equation, it is possible to solve the Hagen-Poiseuille equation for the hydraulic radius, and to estimate the effective pore radius of a cloth from the measured permeability and electrical resistance, as follows:

$$r = (-\frac{8Q\Omega_m}{\tau}\frac{A\kappa\mu}{\Delta p})^{1/2} \qquad (5.4.3)$$

The fractional open area of the pores of tightly woven polyester test fabrics, estimated using the equation (5.4.2) and resistance measurement, is a clear function of both weft density and calendering as shown in Figure 5.4.2. As could be expected, the dependency is stronger with the calendered fabrics, but also the open area of uncalendered fabrics was reduced by increasing the weft density [42].

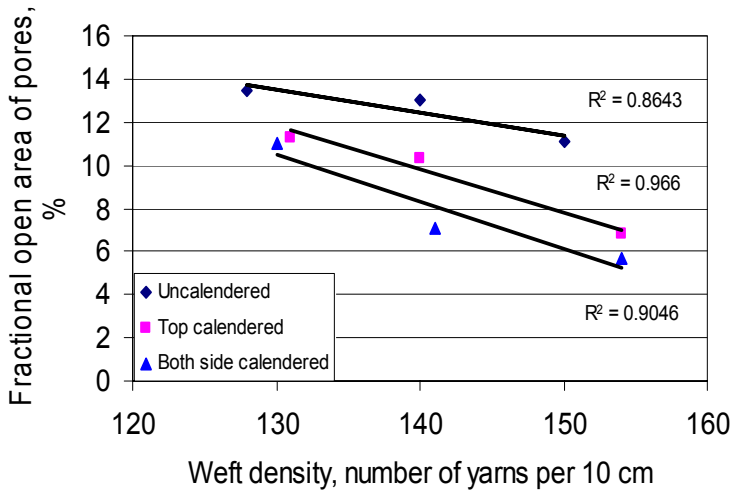

Figure 5.4.2. Estimated fractional open area of pores vs. weft density for the test fabrics.

Both the measured average pore diameter and the bubble point pore diameter seems to be more sensitive to the calendering than to the weft yarn density, as can be seen in figures 5.4.3 and 5.4.4, respectively. This supports the assumption that it is the intra-yarn

pores that account for most of the open area of a tightly woven fabric, and that there exist very few inter-yarn openings in these fabrics. It is likely that calendering closes down the top-most intra-yarn pores very effectively, whereas increasing the number of weft yarns only slightly affects the openings between the yarns because there already exists a maximum number of yarns in the system, and by increasing the number of weft yarns, we only increase the mass of the system. This would also explain the inconsistent behaviour of the average pore size of uncalendered fabrics with respect to the weft density.

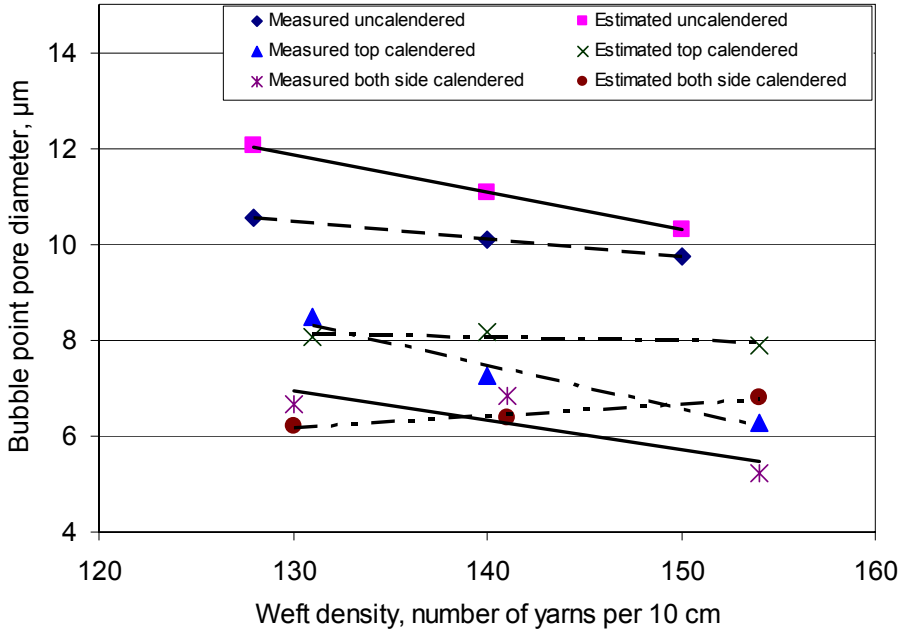

Figure 5.4.3. Measured bubble point pore diameter and estimated pore diameter from air permeability test results vs. weft density for the test fabrics.

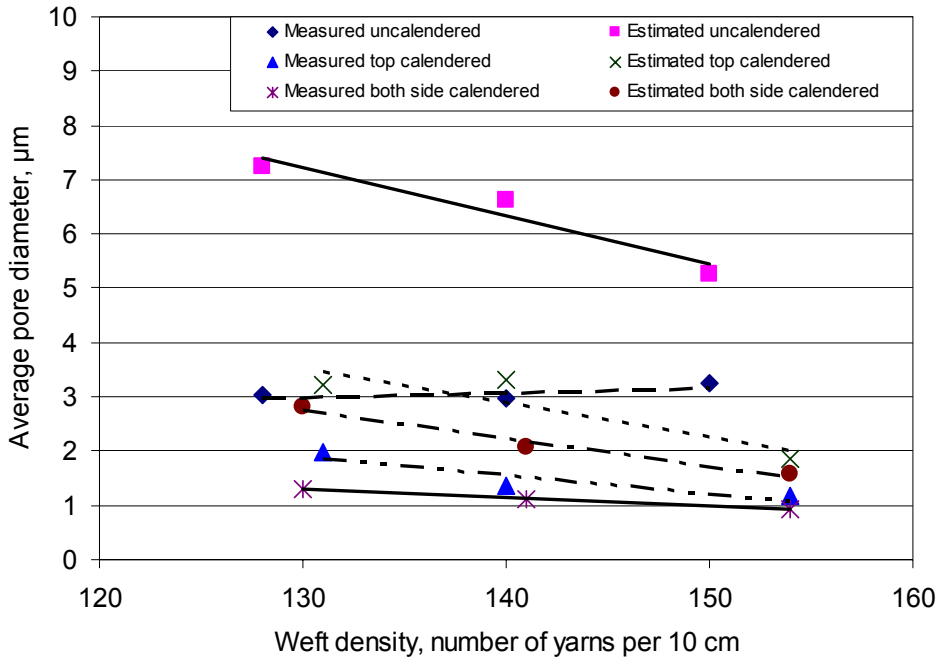

Figure 5.4.4. Measured average pore diameter and estimated pore diameter from water permeability test results vs. weft density for the test fabrics.

In figure 5.4.3 and 5.4.4, the measured bubble point pore diameters and average pore diameters are presented together with the respective pore diameters estimated using formula (5.4.3) and permeability and electrical resistance measurements. For low weft density fabrics, the pore diameters based on air permeability and electrical resistance measurement are consistently lower than the measured values, but for higher weft densities the results are less clear, and it seems that the estimation gives excessively high values for the calendered fabrics. As can be seen from the figures, the estimated pore sizes are very close to the bubble point pore size, which suggests that the bubble point pores (the largest pores) contribute almost 100% of the air flow. The pore sizes calculated using the measured water permeability and electrical resistance values, however, lie somewhere in between the bubble point pore and average pore size, as seen in figure 5.4.4. This finding suggests that water flow through the fabric takes place through the smaller pores. One explanation for this phenomenon may be the higher pressure used in water permeability measurements.

5.5 Testing coated filter cloths

5.5.1 Coated filter media in constant-rate filtration (Paper in Appendix II)

Apart from Lydon's articles [21] [24], there is very little published information on the development and performance of coated solid-liquid filtration media. Thus, the development work for this thesis began by coating standard woven filter fabrics and comparing their performance to that of commercial membranes, namely Desal JX and Koch K602, and to conventional woven filtration cloths.

In the thesis work planned and co-supervised by the author, Toitturi [72] studied the filtration performance of four (4) tightly woven polyester and polypropylene fabrics, one needlefelt fabric, four (4) coated woven fabrics and two commercially available membranes in laboratory-scale dead-end filtration equipment in constant rate filtration mode. The membranes are suitable only for clarification filtration using relatively low pressures in constant rate filtration mode. Consequently, the filtration test conditions and slurries were chosen as described in a conference paper presented in the International Technical Conference on Filtration and Separation in Myrtle Beach, South Carolina. (Appendix II).

The first test slurry was fine-grained lead-zinc ore having an average particle size of 0.43 µm and zeta-potential -22.7 mV (indicating insignificant agglomeration). The second slurry was ultrafine PCC (Precipitated Calcium Carbonate) slurry with an average particle size of 0.50 µm and zeta-potential +11.4 mV (also indicating insignificant agglomeration). The solids concentration for both test slurries was adjusted to 500 ppm. Technical data on the test cloths is presented in table 5.5.1.1.

As can be seen from the test results in table 5.5.1.2., independently of the weave type, the tighter cloths performed better in terms of filtrate clarity and particle retention. The best results were obtained with multi/multi-cloths with fine denier yarns and the poorest performance, in terms of filtrate clarity, with heavier and more open fabrics. For coated fabrics the multi/multi substrate gave the best results, in spite of the fact that the spun yarn substrate-based cloth had lower pure water permeability.

For both membranes, the filtrate was very clear, but the flux was smaller than in the case of fabrics. Compared to the best fabric TF 7, the membranes gave slightly better filtrate clarity, but the required pressure was very high. In addition, the filter cake quality was less attractive for recovery.

The test results confirmed the author's expectations that conventional fabrics can and should be modified to provide the industry with effective microfiltration media, to be used in mineralogical applications where low slurry concentrations are to be filtered. It also became clear, however, that conventional, tightly-woven multifilament cloths with heavy calendaring still produce satisfactory results in terms of filtrate clarity, while providing the most economical dewatering capacity. A disadvantage of coated fabrics and membranes is very high specific resistance, which has to be overcome by high energy input to the system.

Table 5.5.1.1. Technical data of the tested media.

Media	Warp/weft yarn type	Type	Weave	Finish	Planar weight gm^{-2}	Clean medium resistance $10^{10}m^{-1}$
TF 1	Multi/multi	Woven	plain	Heat set	315	0.67
TF 2	Multi/multi	Woven	plain	Heat set + Calendering	320	1.79
TF 3	Multi/spun	Woven	Satin	Heat set + Calendering	550	0.52
TF 4	Multi/multi	Woven	Plain	Heat set + Calendering	380	0.56
TF 5	Multi/multi/ stable fibre	Woven +Needlefelt	Twill	Heat set + Calendering	520	0.68
TF 6	Spun/spun	Woven	Twill	Heat set + PTFE coating	552	11.87
TF 7	Multi/multi	Woven	Twill	Heat set + PTFE coating	455	9.37
TF 8	Mono/mono	Woven	Twill	Heat set +PTFE coating	270	7.47
Ref 9	Koch K602	membrane				
Ref 10	Desal JX	membrane				

Table 5.5.1.2. Constant rate filtration test results.

Media	Filtration resistance at the beginning $10^{11}m^{-1}$	Filtration resistance at the end $10^{11}m^{-1}$	Retention %	Max. Δp kPa	Final Filtrate clarity, FAU
TF 1	2.80	3.09	54	32	250
TF 2	2.88	4.10	90	33	5
TF 3	2.60	2.60	8	30	750
TF 4	2.40	2.80	39	29	500
TF 5	2.52	2.52	6	28	800
TF 6	3.77	5.00	97	46	4
TF 7	2.85	5.86	84	63	0
TF 8	4.00	5.42	48	55	496
Ref 9	3.40	5.00	92	50	0
Ref 10	25.9	17.8	83	60	0

5.5.2 Coated filter media for high-pressure filtration (Paper in Appendix III)

From the results and findings of the developments and testing presented in the previous chapter, it became evident that, in clarification filtration, the membranes outperform the traditional woven and coated cloths in terms of filtrate clarity. In cases where the energy requirement, mechanical strength or media cost are not important issues, the membranes should be the choice. Consequently, this study was focused on high-pressure filtration applications where the media have to have considerable mechanical strength in addition to particle capture capacity. Thus, a new set of trial fabrics was manufactured and tested in a laboratory-scale piston filter descriped in more detail in appendix III. Because the batch filter was built to help in designing the full-scale Tube press filters, which are operated in stepped pressure filtration mode, it was also operated in stepped pressure filtration mode, and the pressure was increased stepwise up to 130 bars.

A typical frame press monofilament cloth was chosen as a reference for the coated and plain fabrics. The planar weight of the reference fabric was 320 g m^{-2}, and the polypropylene warp and weft yarn diameters were 0.15 mm and 0.2 mm, respectively. The test fabric TF201 had a 100 μm thick PU-coating on top of spun yarn woven fabric substrate. The test fabric TF202 had a 20 μm thick PU-coating on top of the substrate, and test fabric TF203 had PU-foam essentially only in the substrate openings. The test fabric TF204 was a plain multifilament woven PES-fabric with heavy calendaring, and test fabric TF205 was a PES multifilament fabric coated on both sides. The planar weights and air permeability of the test fabrics are presented in table 5.5.2.1.

Table 5.5.2.1. Planar weights and air permeability for the test fabrics.

Cloth	Planar weight, g m^{-2}	Air permeability (200 Pa), $m^3m^{-2}min^{-1}$
Reference	320	1.08
TF201	745	0.60
TF202	630	0.94
TF203	650	0.36
TF204	575	0.10
TF205	1145	< 0.06

Figure 5.5.2.1 shows resistance values of all the cloths used in the test filtrations. None of the coated cloths showed a distinct growth of cloth resistance over the duration of the ten filtration cycles.

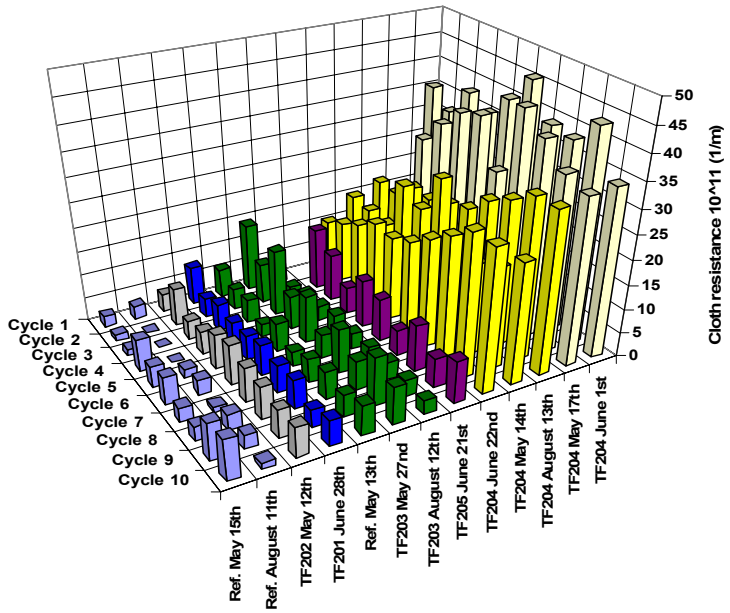

Figure 5.5.2.1. Cloth resistances for the tested cloths.

Throughout the tests, it was evident that the higher the feed solids concentration, the higher the cake solids content compared to the filtrate volume (the solids/filtrate-ratio). Figure 5.5.2.2 shows an example of the impact of feed concentration on the cake solids content/filtrate volume-ratio.

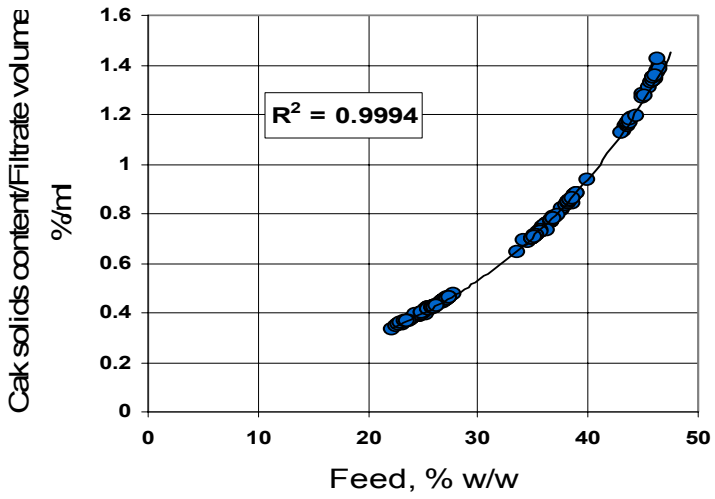

Figure 5.5.2.2. Impact of feed concentration on the cake solids content/filtrate volume-ratio.

From Figure 5.5.2.2 it was concluded that the feed concentration is the main factor affecting the solids content of the cake. The porosity of the cake at the end of the test, however, is not constant, but affected by cake thickness. Figure 5.5.2.3 shows the impact of cake thickness on solids content.

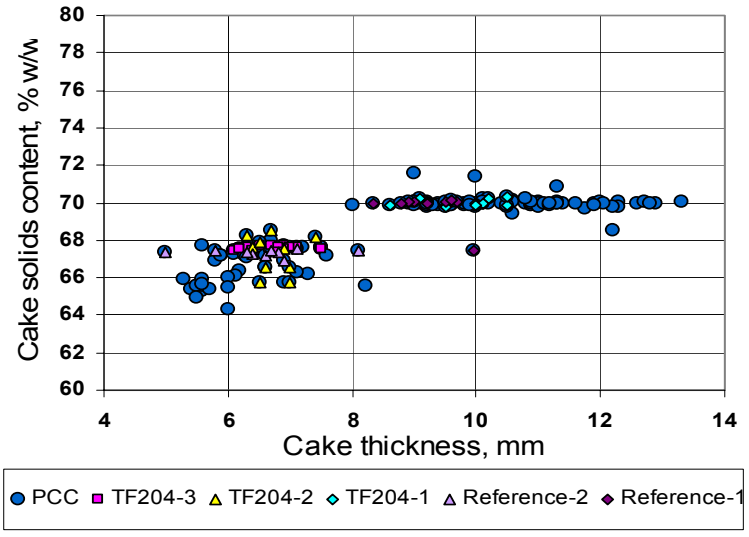

Figure 5.5.2.3. Impact of cake thickness on solids content for all test cloths.

Figure 5.5.2.3 shows that the cake thickness must be more than 8 mm when the targeted solids content in PCC filtration is 70 %. In cases when the solids content in cakes thicker than 8 mm was less than 70 %, the thickness measured in the tests was below the theoretical cake thickness L_c calculated from the filtration test results

$$L_c = \left(\frac{m_{wc} / m_{dc} - 1}{\rho} + \frac{1}{\rho_s} \right) \frac{cV}{A} \qquad (5.5.2.1)$$

where m_{wc} and m_{dc} are the mass of wet and dry cake respectively and ρ_s the density of the solids.

Figure 5.5.2.4 shows estimated capacities for trial filter with PCC slurry. Owing to the structure of the filter, the filling of the filtration chamber into standard slurry volume proved very difficult in practice. Moreover, the volume of the filter chamber is small, making any measuring error all the more evident. It was thus concluded that the solids capacity should be used as a basis for cloth comparison.

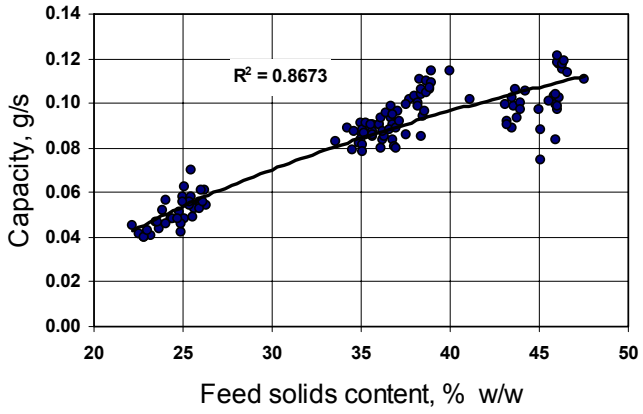

Figure 5.5.2.4. Capacity vs. feed solids content.

As explained in publication in appendix III the initial volumes of the test batches varied slightly from one test run to another. Consequently, in order to be able to compare the test fabric performances from one test to another the filtrate volumes collected were equalized

by dividing them with the initial batch volume. The equalised filtrate volume as a function of time are presented in figure 5.5.2.5.

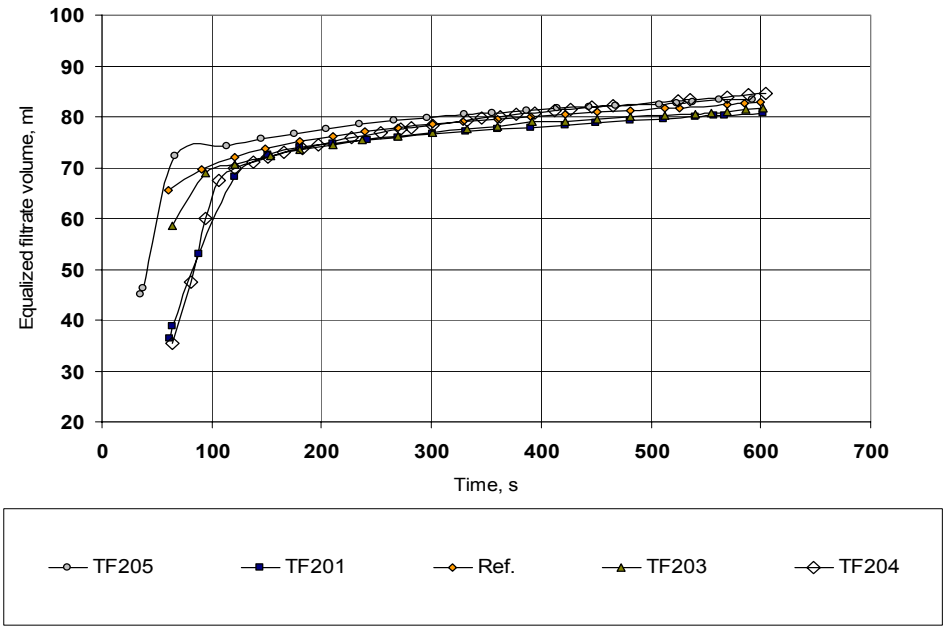

Figure 5.5.2.5. Equalised filtrate volume as a function of filtration time.

In the tests, the compression stage starts after roughly two minutes of filtration. The filtrate volume increase slows down for all the cloths and the initial difference in filtrate volume accumulation evens out. It seems that, during compression, the tightest coated cloth TF205 and also the woven TF204, which has higher cloth resistance, perform slightly better than the others, eventually producing slightly more filtrate than the mono/mono reference cloth.

The clearest difference between the reference cloth and the tested cloths was found in the filtrate clarity as seen in figure 5.5.2.6. When the solid content of the reference cloth filtrate was 22 g/l it was clearly below 2 g/l for all other test cloths. Among the cloths tested, TF203 and TF202 were similar in performance. Cloth resistances were about the same at all feed concentrations, and the filtrate was slightly cloudy in both. If the clarity of the

filtrate is an issue, it is clear that all the test cloths performed clearly better than the reference cloth. More accurate comparison of the test cloths requires further testing because the impact of different cloths on cake release and cloth lifetime was not researched in this study.

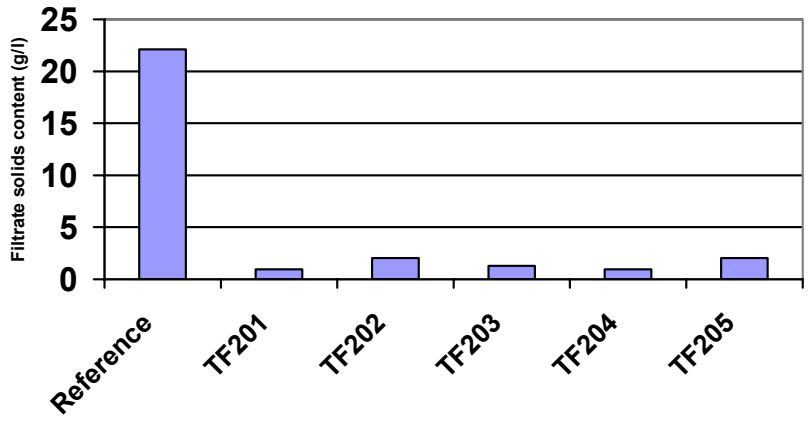

Figure 5.5.2.6. Solids content of filtrate for test fabrics for 10 filtration cycles.

It was concluded that a more accurate comparison of the test cloths requires further testing, because the impact of different cloths on cake release and cloth lifetime was not researched in this study. Moreover, the aim of this work was not to optimise the filtration cycle. The same pressure profile and test time were applied in all test runs. In practice, the operating parameters of a filter have a tremendous effect on the end result of the filtration process, and the cloth performance is also affected.

5.6 Developing dirt-repellent fabrics for pulp de-inking processes (Paper in Appendix IV)

The paper in Appendix IV contains a description of the work done in the R&D department of Tamfelt Corporation's Filter Fabrics Division, to develop and test a dirt-repellent filtration fabric for the de-inked pulp dewatering process.

All tested filter media were weaved and finished to meet the technical specification of a traditional polypropylene monofilament filter bag for a disc filter named Test 1 fabric. This 2/1-twill-weave monofilament fabric has been used in pulp and paper mills for decades, and has proven to be a real all-around fabric for pulp dewatering operations. Altogether there were six different kinds of fluoropolymer blended polyester and other monofilament yarn fabrics, and seven different chemically-treated fabrics manufactured for this study. The performance of these fabrics was compared with the conventional polypropylene, polyester and polyvinylidene fluoride monofilament yarn fabrics. Test fabric technical data is presented in tables 5.6.1 (a) and (b).

Table 5.6.1. (a). Test fabric raw materials.

Fabric id.	Polymer type
Test 1	PP
Test 2	PVDF
Test 3	PBT
Test 4	Modified PET
Test 5	Modified PET
Test 6	PFA
Test 7	ECTFE
Test 8	PET

Table 5.6.1 (b). Chemical treatments for the woven test fabrics.

Fabric id.	Substrate polymer type	Chemical treatment type
Test 1 + treatment A	PP	Silicone
Test 3 + treatment A_1	PBT	Silicone (lower temp.)
Test 3 + treatment A_2	PBT	Silicone
Test 8 + treatment A	PET	Silicone
Test 8 + treatment B	PET	Polyvinylidene fluoride
Test 8 + treatment C	PET	Aqueous dispersion of hydrophilic copolymer manuf. A
Test 8 + treatment D	PET	Aqueous dispersion of hydrophilic copolymer manuf. B

The filtration performance of the test fabrics was measured by a standardised Dynamic Drainage Analyser and related methods. Two different pulps from two different de-inking mills were used for the testing. The Dynamic Drainage Analyser meets the requirements for a reliable method to evaluate pulp slurry drainage at relatively low solids content, under turbulent hydrodynamic conditions. The drainage time is measured as the time from the start of the run until air starts being sucked through the medium. This gives a vacuum curve as a function of time from the start of the test, the dewatering rate being determined from this curve. With the exception of the fabric type, all variables affecting the time required to reach the dry line, that is to say, vacuum pressure, sample volume, consistency, temperature, type of stock and chemicals were all kept constant.

The air permeability value was automatically measured by the Dynamic Drainage Analyser and expressed in pressure units (bars). The resulting cake was subjected to auxiliary analysis such as cake release, cake solids content and dry weight. The filtrate was subjected to analysis such as filtrate clarity (NTU), solids content and ash content.

Based on the filtration performance and the dirt-repellence results of the test fabrics, the best two test fabrics and the three reference fabrics were chosen for the

hydrophilicity/hydrophobicity comparison. The degree of a fabric hydrophilicity/ hydrophobicity was evaluated by measuring the contact angle with a test liquid. In this study, the contact angle was determined by dropping a drop of water onto the fabric surface and then visually evaluating the contact angle between the droplet and the fabric apparent surface.

Results from the Dynamic Drainage Analyser, Dirt-Repellence Tester and Contact Angle Determination test runs are presented in table 5.6.2 (a) and (b) together with the polypropylene, polyester and polyvinylidene fluoride reference fabric results.

Table 5.6.2 (a). Averaged Dynamic Drainage Analyser test results.

Fabric id.	Drainage time, [s]	Air permeability, [bar]	Cake release, [-]	Cake solids content, [% w/w]	Cake ash content, [% w/w]	Cake weight, [g/m^2]
Test 1	6.6	0.356	poor	25.1	7.9	383
Test 1 + treatment A	6.9	0.368	good	26.2	8.0	389
Test 2	6.2	0.318	Moderate	24.4	8.2	385
Test 3	6.9	0.369	poor	25.3	7.7	394
Test 3 + treatment A_1	6.9	0.376	good	26.4	7.9	387
Test 3 + treatment A_2	7.6	0.383	good	27.3	8.1	389
Test 4	7.7	0.339	Moderate	24.8	8.4	387
Test 5	7.6	0.337	Moderate	25.0	8.4	384
Test 6	5.2	0.295	good	25.0	8.0	381
Test 7	7.4	0.352	good	25.1	8.1	382
Test 8	7.5	0.352	Moderate	25.1	8.1	381
Test 8 + treatment A	7.6	0.359	good	25.5	8.1	382
Test 8 + treatment B	7.2	0.346	good	25.7	7.9	378
Test 8 + treatment C	7.1	0.367	Moderate	25.2	8.7	380
Test 8 + treatment D	7.0	0.364	Moderate	25.1	8.3	383

Table 5.6.2 (b). Averaged Dynamic Drainage Analyser test results (continued).

Fabric id.	Filtrate clarity, [NTU]	Filtrate solid content, [g/l]	Filtrate ash content, [% w/w]	Dirt repellence index, [-]	Contact angle [°]
Test 1	331	0.261	43.2	1.16	108
Test 1 + treatment A	317	0.225	45.4	0.16	-
Test 2	345	0.232	46.5	ref.	87
Test 3	329	0.225	46.0	0.90	-
Test 3 + treatment A_1	321	0.240	51.6	0.18	-
Test 3 + treatment A_2	309	0.230	38.7	0.15	-
Test 4	335	0.248	45.6	0.94	-
Test 5	338	0.240	51.5	0.74	78
Test 6	334	0.250	45.5	1.40	-
Test 7	357	0.250	44.6	1.66	-
Test 8	370	0.273	42.2	0.94	74
Test 8 + treatment A	336	0.249	43.2	0.71	-
Test 8 + treatment B	379	0.358	32.8	0.21	-
Test 8 + treatment C	326	0.277	39.2	0.19	-
Test 8 + treatment D	336	0.307	39.2	0.00	24

Measured dirt-repellence indices and selected contact angles for test fabrics and treatments are shown in the graphs 5.6.1 and 5.6.2.

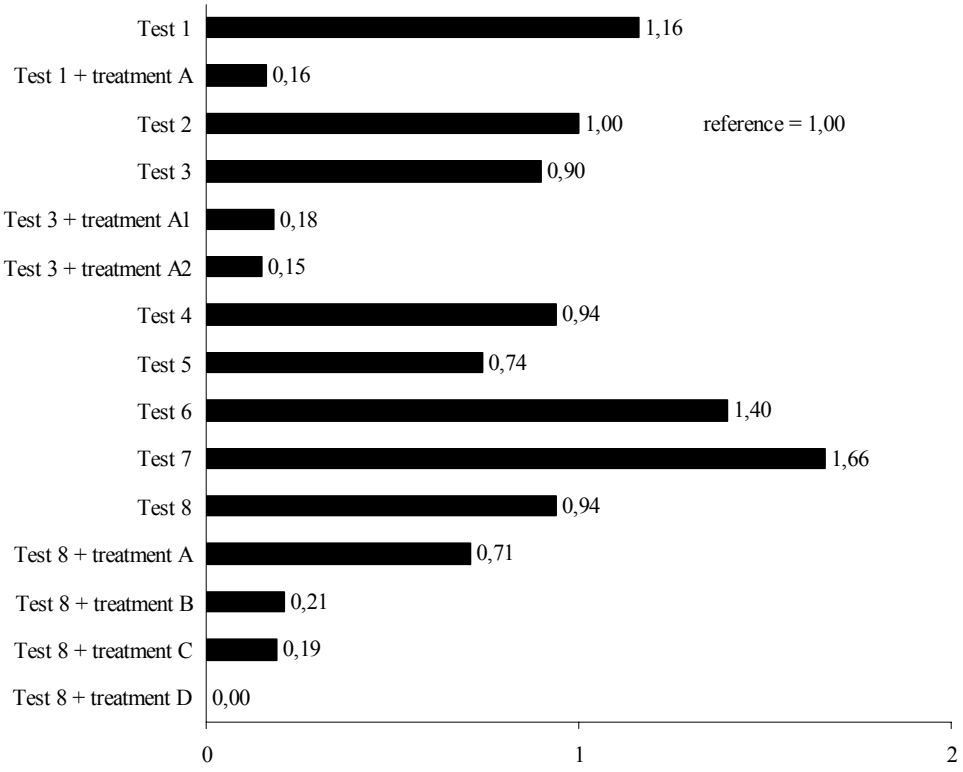

Graph 5.6.1. Dirt-repellence indices for test fabrics.

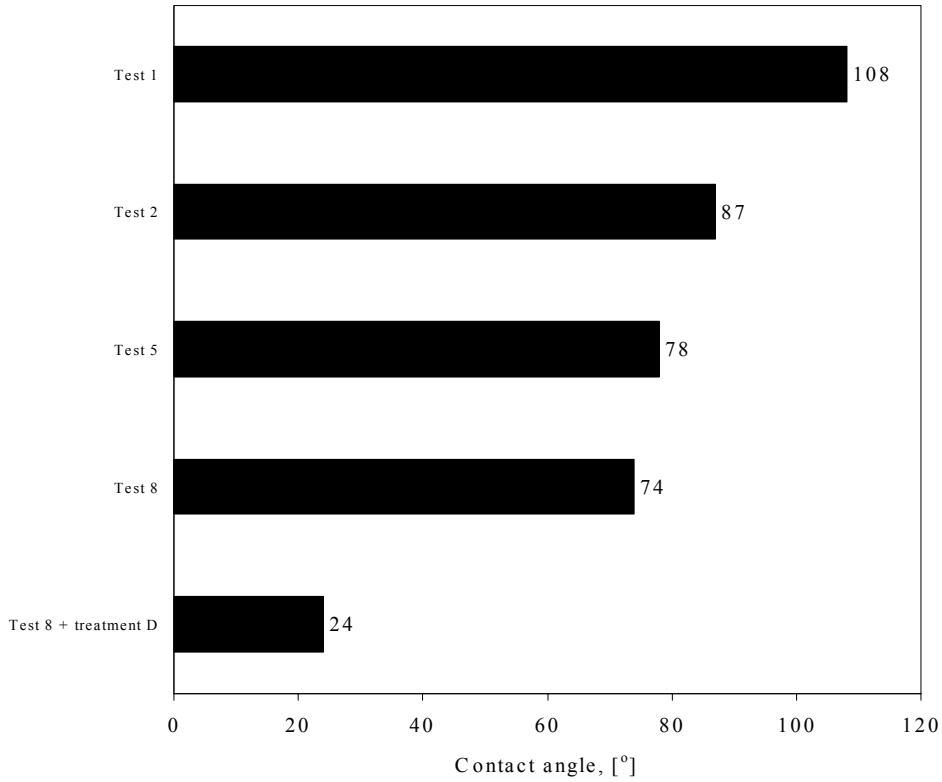

Graph 5.6.2. Contact angles for selected test fabrics and treatment D.

As a conclusion, it seems obvious that chemical treatment produces better results than the use of blended yarns. Many of the fabrics woven of blended yarns performed even worse than the traditional polyvinylidene fluoride fabric in terms of dirt-repellence. The filtration performance analyses indicate that there is no major difference between the drainage time and most other characteristics, with the exception of Test 6 fabric, which was made by blending tetrafluoroethene and perfluoromethylvinylether. Unfortunately the dirt-repellence of this fabric was not as good as with the reference polyvinylidene fluoride fabric.

By far the best dirt-repellence was found with the test fabric 8, which was treated with aqueous dispersion of hydrophilic copolymer. With approximately average filtration performance, this seems to be the choice for low stickies' attachment to the fabric. Surprisingly enough, the test fabric 8 treated with polyvinylidene fluoride (treatment B) gave very poor results in terms of filtrate clarity, although the dirt-repellence was good. It

was assumed that the treatment B somehow lets the solids pass the fabric more easily than other test fabrics.

5.7 Manufacturing and testing polyaniline-treated polyester fabrics for the nickel electrowinning process (Papers in Appendixes V, VI and VII)

To test the performance of the new polyaniline-based coating treatment described in the patent application in Appendix V, a woven PET multifilament reference fabric B was treated with polyaniline to produce the test fabric A. Reference fabric B had a planar weight of 581 g m^{-2} and the measured air permeability was 0.27 $m^3m^{-2}min^{-1}$ (at 200 Pa). The polyaniline-coated fabric A had a slightly higher weight, 585 g m^{-2} and slightly lower air permability 0.23 $m^3m^{-2}min^{-1}$due to the polyaniline treatment. Both fabrics were 0.71 mm thick while the measured porosity (see Appendix I for the testing method) of fabric A was 0.41 and fabric B 0.42. Yet the electrical resistance of fabric A was 40 % less than that of fabric B due to the polyaniline tretament.

Firstly, the polyaniline-treated test fabric A was subjected to standard textile weathering tests described in detail in Appendix VI, to make sure that the treatment is able to withstand normal cloth-handling conditions without losing its characteristics.

Secondly, the fabrics performance in terms of power consumption per nickel tonne produced was tested for three different levels of hydrostatic head in a laboratory-scale polycarbonate cathode-anode cell equipped with the necessary instrumentation. The cell and testing procedure are described in detail in Appendix VII.

In an industrial scale nickel electrowinning operation, there is a continuous feed of nickel sulphate solution to the cathode compartment and pH control to keep the process condition optimal for nickel reduction. In the experimental cell, it was found that, in order to be able to compare the performance of two different fabrics, it is necessary to test the

fabrics for several different levels of hydrostatic head, in order to be able to interpolate the hydrostatic head levels, which give equal electrolyte flow through the fabric.

The electrolyte used in the experiment was a commercial-grade nickel electrowinning process electrolyte with initial pH 2.8 and initial nickel concentration of 136 g/l. There was practically no sulfuric acid present in the initial electrolyte, and only minor concentrations of other components. The test cell operation efficiency was measured in terms of a potential drop across the diaphragm, the cell voltage, bulk-flow through the diaphragm, anolyte and catholyte ionic concentrations before and after the test runs, and gravimetric nickel production for three (3) different hydrostatic heads. In addition, the anolyte and catholyte pH and conductivities were measured before and after each test run.

The measured average electrolyte flow through the diaphragm, average cell voltage, average potential drop across the diaphragm and total amount of reduced nickel for each test are presented in table 5.7.1.

Table 5.7.1. Average flow through the diaphragm, cell voltage, potential drop across the diaphragm, electrolytic nickel production and calculated current efficiencies for the test runs.

	Diaphragm A			**Diaphragm B (ref.)**		
Hydrostatic Head, cm	3	5	10	3	5	10
Flow through diaphragm, ml/h	3.96	16.17	42.46	21.79	39.83	87.92
Cell voltage, mV	4956	5173	5311	5321	5724	5945
Diaphragm potential drop, mV	602 (12 %)	658 (12.7 %)	762 (14.3 %)	785 (14.8 %)	1246 (21.8 %)	1300 (21.9 %)
Produced nickel, grammes	49.12	49.81	52.18	51.46	52.82	53.04

Flow through the diaphragm and current efficiency from table 5.7.1 are plotted against the hydrostatic head in figures 5.7.1 and 5.7.2.

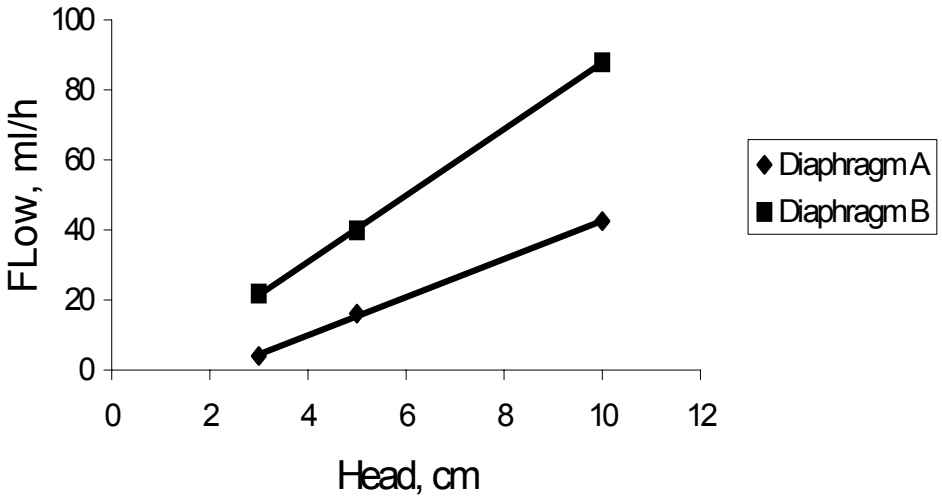

Figure 5.7.1. Flow through the diaphragm vs. three different levels of hydrostatic head for diaphragm fabrics A and B.

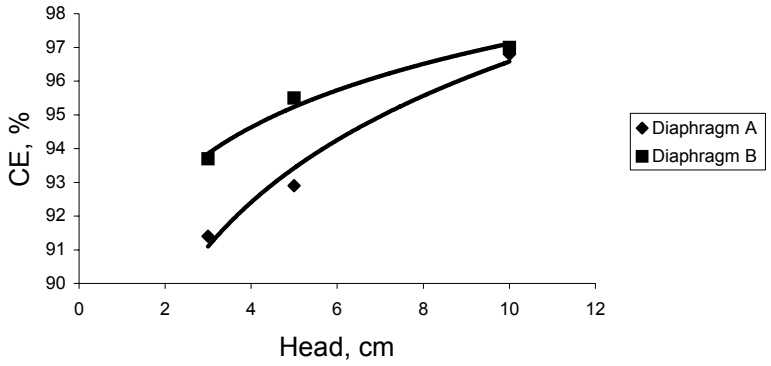

Figure 5.7.2. Current efficiency (CE) vs. three different levels of hydrostatic head for diaphragm fabrics A and B.

Analysed ionic concentrations before and after each test run allow calculation of the total ionic fluxes through the diaphragm within the 24-hour run. These fluxes are presented in figures 5.7.3 to 5.7.5.

As can be seen in figure 5.7.1, having a high hydrostatic head means a high flow through the diaphragm. For the more open reference fabric B, the flow was significantly higher also resulting in higher flux of sulphate and nickel through the fabric as can be seen in figures 5.7.3 and 5.7.4. As can be seen in figure 5.7.5, the hydrogen flux was also clearly higher than with the polyaniline-coated fabric A with lower porosity.

As explained by Sermyagina *et al.* [68], there exists a critical level of hydrostatic head for a given diaphragm, which prevents the influx of hydrogen to the cathode compartment. In fact, the only case in which the hydrogen ions did not flow from the anode to the cathode in the case of fabric A was with a 10 cm head. Consequently, the comparison between fabric B and the new fabric A was based on the test case where the hydrostatic head for diaphragm fabric A was 10 cm, and measured flow through the fabric was 42.46 ml/h.

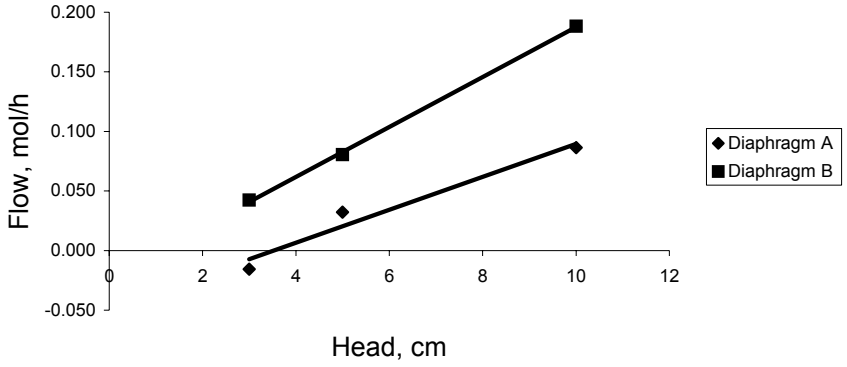

Figure 5.7.3. Nickel flow through the diaphragm vs. three different levels of hydrostatic head for diaphragm fabrics A and B.

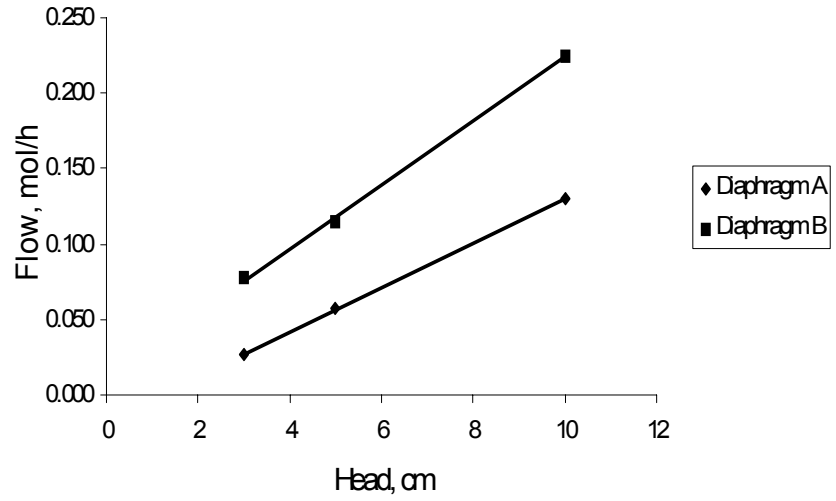

Figure 5.7.4. Sulphate flow through the diaphragm vs. three different levels of hydrostatic head for diaphragm fabrics A and B.

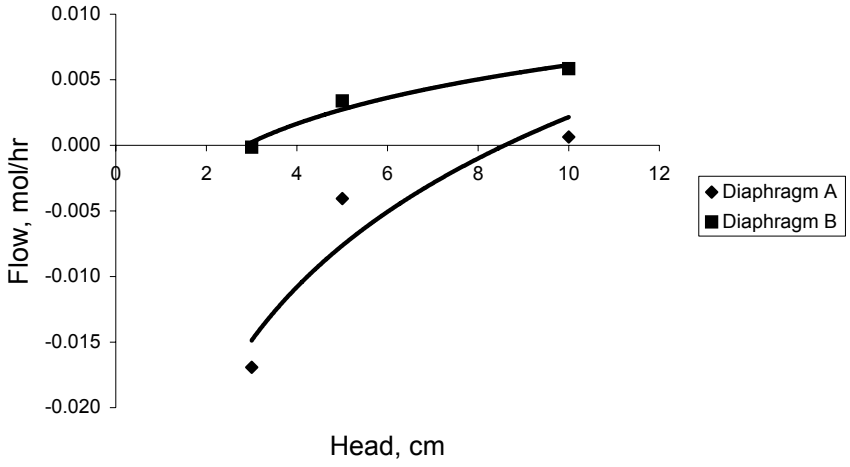

Figure 5.7.5. Hydrogen flow through the diaphragm fabric vs. three different levels of hydrostatic head for diaphragm fabrics A and B.

Process performance values for reference fabric B for the operating flow of 42.46 ml/h through the diaphragm fabric were then estimated by fitting the table 5.7.1 performance results against the measured flow rates, and interpolating the 42.46 ml/h flow rate performance values. Graphical presentations of the main performance characteristics for the reference fabric B together with the fitting results are presented in figures 5.7.6 and 5.7.7.

Comparison of the two diaphragm fabrics performance at the selected operating point is presented in table 5.7.2.

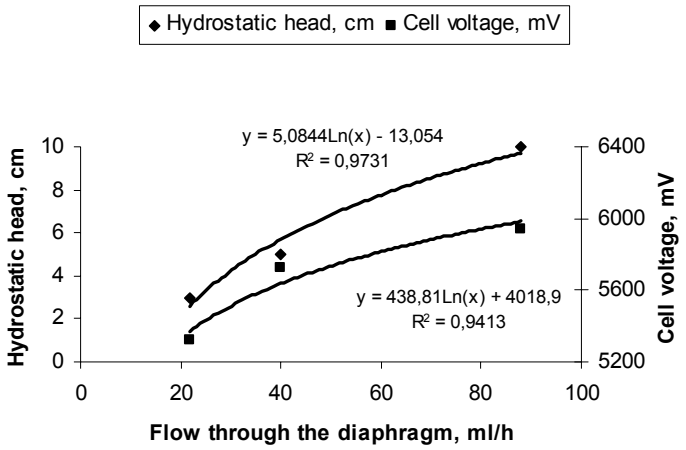

Figure 5.7.6. Reference fabric B hydrostatic head and cell voltage vs. flow through the diaphragm fabric.

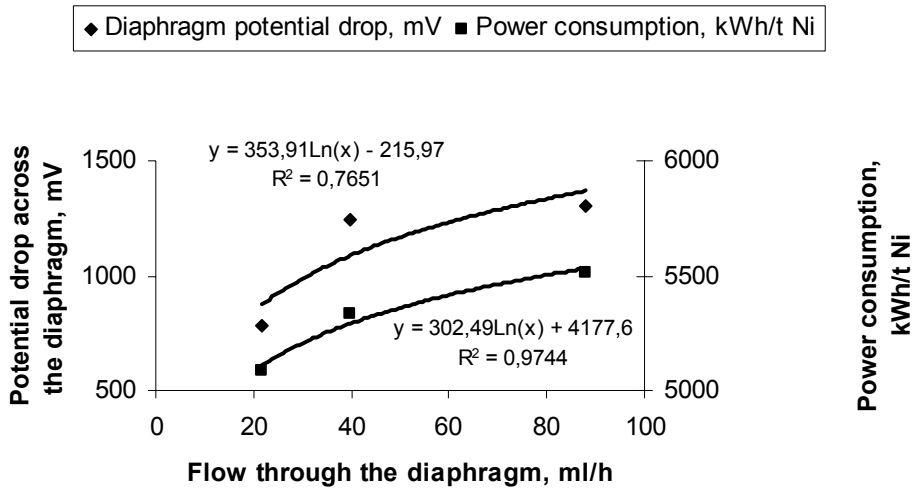

Figure 5.7.7. Reference fabric B nickel production and current efficiency vs. flow through the diaphragm fabric.

Table 5.7.2. Average flow through the diaphragm, cell voltage, potential drop across the diaphragm, electrolytic nickel production and calculated current efficiencies for the test runs.

	New diaphragm A	**Reference diaphragm B** **(interpolated values)**
Flow through diaphragm, ml/h	42.46	42.46
Hydrostatic Head, cm	10	6
Cell voltage, mV	5311	5664
Diaphragm potential drop, mV	762 (14.3 %)	1111 (19.6 %)
Power consumption, kWh/t Ni	5008	5312

As can be seen in table 5.7.2, the new polyaniline-coated diaphragm fabric A performs better than reference fabric B in terms of power consumption per tonne of nickel produced. This is because both the cell voltage and potential drop across the diaphragm are lower

than with the more permeable reference fabric B. From this test, it can be concluded that, for nickel production, fabric A consumes less energy than the conventional fabric B. The absolute amount of nickel produced is almost the same for both fabrics, and the only difference is the higher hydrostatic head with fabric A.

6. Conclusions

The main aim of this thesis work was to develop and test various coatings and treatments for the most common woven media used in selected liquid filtration applications. The performance of the coated or chemically- and thermally-treated media was compared to the respective woven cloth performance used in laboratory-scale filtration tests.

For the filtration of PCC slurry, several coatings and treatments were developed and tested, both in constant rate and stepped pressure filtration modes, as opposed to the plain woven media performance.

For de-inked pulp dewatering applications, the commercially-available dirt-repellent chemical treatments and specially blended yarns were tested in order to verify their effectiveness vis-à-vis the non-treated cloths.

Finally, a new method of applying polyaniline coating on top of a standard multifilament cloth for the nickel electrowinning process was developed and tested in terms of performance.

The results achieved by various chemical surface treatments clearly show that the surface properties of woven media can be modified to achieve lower electrical resistance and better dirt-repellency than the present state-of-art commercial plain woven fabrics have. Technically, the main challenge with the chemical treatments is the abrasion resistance of the treatment, and while the weathering experiment results indicate that the treatment is sufficiently permanent to resist standard handling operations, it is still possible that the treatment is inadequately strong for actual use. The testing in this respect is continuous and it will be possible to draw final conclusions only after years of industrial use.

Based on the pressure filtration studies, it seems obvious that the conventional woven multifilament fabric still performs surprisingly well against the new coated media in terms of filtrate clarity and cake build-up. Especially in cases where the feed slurry concentration is low, the conventional media seem to outperform the coated media. In the cases where the

feed slurry concentration was high, the tightly woven media performed well against the monofilament-based fabrics but seemed to do worse than the coated media. This result is somewhat surprising in that the high initial specific resistance of the coated media would suggest that the media should blind more easily than the plain woven media. The results indicate, however, that it is actually the woven media that gradually clogs during the course of filtration. In conclusion, it seems obvious that there is a pressure limit above which the woven media loses its capacity to keep the solid particles from penetrating the structure.

This finding also suggests that, for extreme pressures, the only foreseeable solution is coated fabrics supported by a sufficiently strong woven fabric to hold the structure together. The experimental results show that some coatings, but not all, perform better than the tightly-woven fabrics in terms of long-term flow resistance. However, the stepped high pressure filtration process seems to follow somewhat different laws to the more conventional processes. Based on these results, it may well be that the role of the cloth is most of all to support the cake, and the main performance determining factor is the long life time.

In this study, the economical aspects of coating and treatment applications were not studied. Naturally the overall economics have to be looked at carefully before the proposed treatments can be widely used in the process industry.

During the development work of the treatments, a new method of estimating the effective pore size and open pore area in a densely woven multifilament fabric was developed. The results were validated by comparing them to the measured values of the largest pore size (Bubble point) and the average pore size using an industrial porometer.

The results indicate that it would be potentially possible to use the standardised permeability and electrical resistance methods to estimate the total open pore area and hence the effective pore diameter of media. In order to have the proposed method in standard use, however, it is necessary to make a comparative study between various existing industrial pore size analysis methods and the proposed method. Another obvious deficiency of the developed method is the assumption that the electrical resistance of a solid material is infinitively high. This limits the use of the developed model at this point to

the comparative use of media manufactured using exactly the same raw material, until the possible differences in electrical resistances of solid material can be taken into account by the method.

7. References

1. Mayer, E., Cake filtration theory and practise, Chemical Engineering Journal, Vol 80(2000), pp 233-236.
2. Tiller, Frank M., What the filter man should know about theory, Filtration (Special Issue), April 2004, pp 55-67.
3. Wakeman, R.J., Tarleton, E.S., Filtration, Equipment selection, modelling and process simulation, Elsevier Advanced Technology, Oxford, 1999.
4. Horrocks, A.R. and Anand, S.C., Handbook of technical textiles
5. Adanu, S., Wellington Sears Handbook of Industrial Textiles, CRC Press, 1995.
6. Purchas, D., Handbook of filter media, 1st edition, Oxford, Elsevier Advanced Technology, 1996.
7. Rushton, A., Ward, A.S., Holdich, R.G., Solid-Liquid Filtration and Separation Technology, 1st edition, Mörlenbach, VCH Publishers, 1996.
8. Lu, W-M., Tung, K-L., Hweng, K-J., Effect of woven structure on transient characteristics of cake filtration, Chemical Engineering Science, Vol. 52 (1997), No 11., pp. 1743-1756.
9. Rusthon, A. and Rushton, Alan, Size and concentration effect in Filter cloth pore bridging, Filtration & Separation, may/june 1972, pp 274-278.
10. Booth, J.E., Textile Mathematics, The textile Institute, 1977, Manchester.
11. Epps, HH., Leonas, KK., The relationship between porosity and air permeability of woven textile fabrics, Journal of testing and evaluation, Vol. 25, No 1., 1997, pp 108-113.
12. Kienbaum, M., Gewebegeometrie und Producktentwicklung, Melliand Textilberichte, 11/1990, pp 847-854.
13. Militky, J., Travnickova, M., Bajzik, V., Air permeability and light transmission of weaves, IJCST Vol. 11(1999), No 2/3, pp 116-124.
14. Pierce, F.T., The geometry of cloth structure, The Journal of the Textile Institute, Transactions, March 1937, pp 45-96.

15. Järvinen K., A novel technique for estimating the effective pore size and open area for densely woven filter fabrics, Filtration, 5(2), 2005, pp.126-133.
16. Hardman, E., Filter media selection, science or black art, J.Filt.Soc., Vol 2(1), 2001, pp 11-14.
17. Hardman, E., Some aspects of the design of filter fabrics for use in solid/liquid separation processes, Filtration+Separation, Vol 31(1994), No 10., pp 813-818.
18. Barlow, G., Haczycki, S.J., Measuring the retention efficiency of fabric filter media, Filtration and Separation Vol. 18(1981), No. 6 Nov-Dec., pp 518-520.
19. Fletcher, E.A., Needled Filter Media for solid/liquid separation, World Filtr.Congr. 1979, (London)2, pp 403-414.
20. Goosens, F., Improvement of surface structure of filter media by bonding, laminating, coating and impregnating, Journal of Coated Fabrics, Vol. 22(1993), April 38, pp 279-289.
21. Lydon, R.P., Filter media surface modification technology: state of the art, Filtration+Separation Vol. 41(2004), November , pp 20-21.
22. Lee, J.K., Liu, B.Y.H., Rubow, K.L., Yoo, S.H., Filtration of real-world particles in liquids by microporous membrane filters, Journal of the IES, Vol. 38(1995), No 3., pp 19-25.
23. Matsuura, T., Synthetic membranes and membrane separation processes, CRC Press 1995, Ontario, Kanada.
24. Lydon, R.P., The development of surface filtration filter media for the improved separation of fine particles in industrial filtration processes, Advances in Filtration and Separation Technology, American Filtration & Separation Society, Vol 14(2000), 5 p.
25. Allen, R., Lydon, R., Johnson, J, Improved abrasion resistant coatings for industrial filtration applications, J.Filt.Soc., Vol. 2(2001), No 1, pp 21-23.
26. Maurer, Ch., Composite membranes for microfiltration in the process industry, F&S International Edition, Vol. (2004), No 4, pp 40-42.
27. McKinney, R.W.J., A review of sticky control methods, including the role of surface phenomena in Control, Tappi Proceedings – Pulping Conference – Book 1, 22-25.10.1989, Tappi Press, Atlanta, USA, pp 177-183.

28. Grottenmüller, R., Fluorocarbone-ein innovatives Hilfsmittel zur Veredlung von textilen Oberflächen, Melliand Textilberichte 10/1998, pp 743-746.
29. Lämmermann, D., Fluorocarbone in der textilen Endausrüstung-Eigenschaften und Anwendungen, Melliand Textilberichte 11/1991, pp 949-954.
30. Carson, R.S., Anti-contaminant dryer fabrics for today's changing environment, PaperAge, February 1996, pp 42-43.
31. Fischer, B., Ein Beitrag zur Verminderung der Anschmutzung von Papiermaschinenbespannungen, Wochenblatt für Papierfabrikation, Vol. 127(1999), Nr. 13, pp 895-900.
32. Sundholm, F., Ledande Plaster, Kemia-Kemi, Vol 28(2001), pp 17-18.
33. Bugnet, B., Costa, M., Doniat, D., Doniat, J., Rouget, R., Products with a porous structure premetallised with electroconductive polymers and process for their preparation, patent EP761710.
34. Järvinen, K., Heikkilä, A-M., Suodatinkangas märkäsuodatukseen, Finnish patent application 20010414.
35. Kuhn, H. H., Olney medal address. Adsorption at the liquid/solid interface conductive textiles based on polypyrrole. Text. Chem. Color. 29 (12), 17-21 (1997).
36. Kuhn, H.H., Kimbrell, W.C., Fowler, J.E., Barry, C.N., Properties and applications of conductive textiles, Synthetic Metals 57 (1), 3707-3712 (1993).
37. Rivas, B.L., Sanchez´, C.O., Synthesis, Characterisation and Electrical Conductivity of Polyaniline Derivatives: Study with the Metal Ions Cu(II), Ni(II) and Co(II). Journal of Applied Polymer Science, Vol. 82, 330-337, 330-336 (2001).
38. Svarovsky, L., Solid-liquid separation, 2ed ed. 1981, Butterworths & Co Ltd.
39. Biswas S. and Winoto S.H., Prediction of pressure drop in non-woven filter media using a Hagen-Poiseuille model, Tribology Transactions 2000 43/2 (251-256).
40. Paterson M.S., The equivalent channel model for permeability and resistivity in fluid-saturated rock- a re-appraisal, Mechanics of Materials 2 (1983), pp 345-352.

41. Dias, R., Mota, M., Teixeira, J.A., Yelshin, A. Study of terniary glass spherical particle beds:porosity, tortuosity and permeability, Filtration 5(1), 2005, pp
42. Brasquet, C., Le Cloirec, P., Pressure drop through textile fabrics-experimental data modelling using classical models and neural networks, Chemical Engineering Science, Vol. 55(2000), pp 2767-2778.
43. Bird, R.B., Stewart, W.E., Lightfoot, E.N., Transport Phenomena, Wiley, New York, 1960.
44. Lu, W.M., Tung, K.L., Hwang, K.J., Fluid flow through basic weaves of monofilament filter cloth, Textile Res.J., Vol 66(1996), pp 311-323.
45. Brundrett E., Prediction of Pressure Drop for Incompressible Flow Through Screens, Journal of Fluids Engineering, June 1993, vol. 115, 239-242.
46. Rushton, A., Griffiths, P.V.R., Role of the cloth in filtration, Filtration (Special Issue) April 2004, pp 47-54.
47. Ripperger S., Strompor M., Fiala P., Experimentelle Methoden zur Charakterisierung der Barrierwirkung von Geweben gegenuber Flussigkeiten und Partikeln, Filtrieren und Separieren, Vol. 16(2002), Nr. 3, 130-137.
48. Takada K., Makabe A., Takaku A., Porosity and air permeability of woven and knitted fabrics, Tokyo Kasei Daikagu Kenkyu Kiyo 2002, No. 42, pp 119-124.
49. Rideal G., Mayer E., Lydon R., Comparative methods for the pore size calibration of filter media, 2004, Filtration, 4(1), pp 29-33.
50. Jena A.K., Gupta K.M., Characterisation of pore structure of filtration media, Fluid Particle Separation Journal, Vol 14(2002), Nr. 3, 227-241.
51. Jena A.K. and Gupta K.M., “Pore Size Distribution in Porous Materials, 1999, Proceedings of International Conference Filtration 99, INDA, Chicago.
52. Jena A.K. and Gupta K.M., “Homogeneity of Pore Structure of Filtration Media”, 2002, Proceedings of the 15th Annual Technical Conference, The American Filtration & Separation Society, April 9-12, Galveston, Texas.
53. Mayer E., Porometry observations, in Advances in Filtration and Separation Technology, Advancing Filtration and Separation Solutionsfor the Millenium, American Filtration & Separation Society, 1999, pp 851-859.

54. Dubrovski, P.D., Brezocnik, M., 2002, Using Genetic Programmeming to Predict the Macroporosity of woven Cotton Fabrics, Textile Research Journal, 72 (3): 187-194.
55. Rideal G., Storey J., A new high precision method of calibrating filters, J.Filt.Soc., Vol 2(3), 2002, pp 18-21.
56. Oja M., Pressure Filtration of Mineral Slurries: Modelling and Particle shape Characterisation, Doctoral thesis , Lappeenranta 1996.
57. Fathi-Najafi M., Theliander H., Determination of local filtration properties at constant pressure, Separations Technology, 5(1995), pp 165-178.
58. Johansson C., Theliander H., Measuring concentration and pressure profiles in deadend filtration, 2003, Filtration 3(2), pp 114-120.
59. Ingmanson W.L., Whitney R.P., The filtration of pulp slurries, TAPPI 1954, Vol. 37, No. 11, pp 523-533.
60. Leu W.F., Tiller F.M., Cake compactibility-a rigorous definition, 1993, 6th World Filtration Congress, Nagoya, Japan, pp. 148-153.
61. Wakeman R.J., A numerical integration of the differential equations describing the formation of and flow in compressible filter cakes, 1978, TransIChemE, Vol. 56, pp. 258-265.
62. Tarleton E.S., Morgan S.A., An experimental study of abrupt changes in cake structure during dead-end pressure filtration, Trans.Filt.Soc., Vol 1 (4), 2001, pp 93-100.
63. Rainer M., Höflinger W., Experimental and CFD analysis of particle retention on different filter media in solid-liquid filtration, 2002, Trans.Filt.Soc., 2(4), pp 114-119.
64. Awakura, Y., Doi, T., Majima, H., Determination of the diffusion coefficients of $CuSO_4$, $ZnSO_4$, and $NiSO_4$ in aqueous solutions, Metall.Trans.B 19B(1), Feb. 1988, pp 5-12.
65. Chapman, T.W., Characterizing effects of novel hydrometallurgical process chemistry on electrowinning operations, Hydrometallurgical Process Fundamentals, Cambridge UK, 25-31 July 1982.
66. Knuutila, K., Nickel electrolysis process at Outokumpu Harjavalta Metals Oy, 33rd Metallurgical Seminar of the GDMB, Lünen, Germany, November, 1997, pp 19-21.

67. Lenthall, K.C., Bryson, A.W., Electrowinning of cobalt from sulphate solutions, TMS Annual Meeting Feb 9-13 1997, pp 305-320.
68. Sermyagina, K.N., Andrushchenko, V.N., Shmonin, O.I., Optimisation of the nickel content in the catholyte during electrorefining of nickel, Tsvetnye Metally (4), Apr. 1990, pp 37-39.
69. de Kretzer, R.G., Usher, S.P., Scales, P.J., Landman, K.A., Boger, V., Rapid Filtration Measurement of De-Watering Design and Optimisation Parameters, AIChE Journal (2001a), 47(8), pp 1758-1769.
70. Usher, S.P., De Kretser, R.G., Scales, P.J., Validation of a New Filtration Technique for Dewaterability Characterisation, AIChE Journal (2001), 47(7), pp 1561-1570.
71. Tarleton, E.S., Hadley, R.C., The application of mechatronic principles in pressure filtration and its impact on filter simulation, Filtration, 3(1), 2003, pp 40-47.
72. Toitturi, K, Masters thesis work, 1999, Lappeenranta University of Technology, Finland.

Appendices